LA-10105-OBES

Los Alamos National Laboratory is operated by the University of California for the United States Department of Energy under contract W-7405-ENG-36.

Low-Temperature Geothermal Potential of the Ojo Caliente Warm Springs Area, Northern New Mexico

Los Alamos National Laboratory
Los Alamos, New Mexico 87545

This work was supported by the US Department of Energy, Office of Basic Energy Sciences.

Edited by Glenda Ponder, ESS Division

DISCLAIMER

LA--10105-OBES
DE84 013857

Low-Temperature Geothermal Potential of the Ojo Caliente Warm Springs Area, Northern New Mexico

F. D. Vuataz*
J. Stix**
F. Goff
C. F. Pearson†

*Director's Postdoctoral Appointee at Los Alamos. Institut Mixte de Recherches Géothermiques, BRGM, BP 6009, 45060 Orléans Cedex, FRANCE.
**Graduate Research Assistant at Los Alamos. University of Toronto, Department of Geology, Toronto, CANADA M5S 1A1.
†Present address: KRTA Ltd., CPO Box 4498, Auckland, NEW ZEALAND.

Los Alamos National Laboratory
Los Alamos, New Mexico 87545

CONTENTS

CONVERSION OF UNITS OF MEASUREMENTS

Used in this report	Multiply by	To obtain
Length		
centimeter (cm)	0.3937	inch (in.)
meter (m)	3.281	foot (ft)
kilometer (km)	0.6214	mile (mi)
Surface		
square kilometer (km^2)	0.3861	square mile (mi^2)
Volume		
cubic meter (m^3)	35.31	cubic foot (ft^3)
Flow		
liter per minute (ℓ/min)	0.2642	gallon per minute (gal/min)
cubic meter per second (m^3/s)	15,850	gallon per minute (gal/min)
cubic meter per day (m^3/d)	264.2	gallon per day (gal/d)
Specific capacity		
liter per minute per meter (ℓ/min•m)	0.0805	gallon per minute per foot (gal/min•ft)
Transmissivity		
square meter per day (m^2/d)	10.76	cubic foot per day per foot (ft^3/d•ft)
Temperature		
degree Celsius (°C)	1.8 (+ 32)	degree Fahrenheit (°F)
Heat flow		
milliwatt per square meter (mW/m^2)	0.0239	heat flow unit (HFU)
Electrical conductivity		
microsiemens per centimeter (μS/cm)	1.000	micromho per centimeter (μmho/cm)

LOW-TEMPERATURE GEOTHERMAL POTENTIAL OF THE OJO CALIENTE WARM SPRINGS AREA, NORTHERN NEW MEXICO

by

F. D. Vuataz, J. Stix, F. Goff, and C. F. Pearson

ABSTRACT

The Ojo Caliente area is characterized by north-trending Precambrian horsts unconformably overlain by Miocene fluvial basin-fill sediments that dip gently to the southeast. North-south facies changes are common within the Miocene section. These sediments are in turn unconformably overlain by flat-lying to gently dipping Quaternary terraces, travertine, loess, and alluvium. Geothermal manifestations in the study area are controlled primarily by normal faulting that offsets the Precambrian and Tertiary sections.

A detailed geochemical investigation of 17 waters (thermal and cold, mineralized and dilute) was performed in the Ojo Caliente-La Madera area. Two types of thermomineral waters have separate and distinctive geologic, geochemical, and geothermal characteristics. The water from Ojo Caliente Resort emerges with temperatures $\leq$54°C from a Precambrian metarhyolite. Its chemistry, typically Na-HCO_3, has a total mineralization of 3600 mg/ℓ. Isotopic studies have shown that the thermal water emerges from the springs and a hot well without significant mixing with the cold shallow aquifer of the valley alluvium. However, the cold aquifer adjacent to the resort does contain varying amounts of thermal water that originates from the warm spring system. Geothermometry calculations indicate that the thermal water may be as hot as 85°C at depth before its ascent toward surface. Thermodynamic computations on the reaction states of numerous mineral phases suggest that the thermal water will not cause major scaling problems if the hot water is utilized for direct-use geothermal applications. By means of a network of very shallow holes, temperature and electrical conductivity anomalies have been found elsewhere in the valley around Ojo Caliente, and resistivity soundings have confirmed the presence of a plume of thermal water entering the shallow aquifer.

The group of lukewarm springs around La Madera, with temperatures $\leq$29°C, chemical type of NaCaMg-HCO_3,Cl and with a total mineralization $\leq$1500 mg/ℓ behaves as a different system without any apparent relation to the Ojo Caliente system. Its temperature at depth is not believed to exceed 35-40°C.

The geothermal potential of Ojo Caliente seems to be interesting not only because the water could reach 85°C at depth but

also because large volumes of thermal water are continuously discharging into the valley alluvium from concealed fissures in the metarhyolite. More detailed geophysical studies and two or three slim exploratory drill holes could ascertain the local geothermal potential in a quantitative way. Thus, low-temperature geothermal applications could be considered for Ojo Caliente, such as space heating for buildings and greenhouses.

---

1. INTRODUCTION

The Ojo Caliente warm springs area (Fig. 1) is located at the boundary between Rio Arriba and Taos counties, in north-central New Mexico, 75 km south of the Colorado border and 60 km northeast of the Valles Caldera. Ojo Caliente itself is a small community built around an old spa that is still active. In 1534, the warm springs of Ojo Caliente were visited and named by Cabeza de Vaca, an early explorer of New Mexico. These springs have been used as a spa for many years and were first mentioned in the geologic literature in 1875 (Summers 1976).

The purpose of the present study is to assess the low-temperature geothermal potential of the Ojo Caliente area and to determine (1) if more water is available at depth than that naturally discharged, (2) if one can tap hotter water, and finally, (3) if the thermal water anomaly is concentrated around the resort itself or is spread over a wider area. Warm water resources would be very useful in a small community like Ojo Caliente or La Madera for space heating of buildings and greenhouses (Ungemach 1982). To answer these hypotheses, the geology of the area around Ojo Caliente has been compiled and mapped, the geochemistry of all waters, thermal and cold, ground and surface, from Ojo Caliente to La Madera has been assessed, and a shallow-hole temperature network and a resistivity sounding survey have been completed.

Not much has been written previously on the thermal waters of Ojo Caliente, but earlier research is summarized by Summers (1976) in his "Catalog of Thermal Waters in New Mexico." The Bureau of Land Management in Albuquerque (1978) prepared an "Environmental Assessment Record and Technical Examination on Proposed Geothermal Leasing in the Ojo Caliente Area." The proposed action was to offer, for geothermal leasing, about 552 km^2 of public land in the Rio Arriba and Taos Counties. This report mostly concerns description of the existing local environmental conditions and the possible

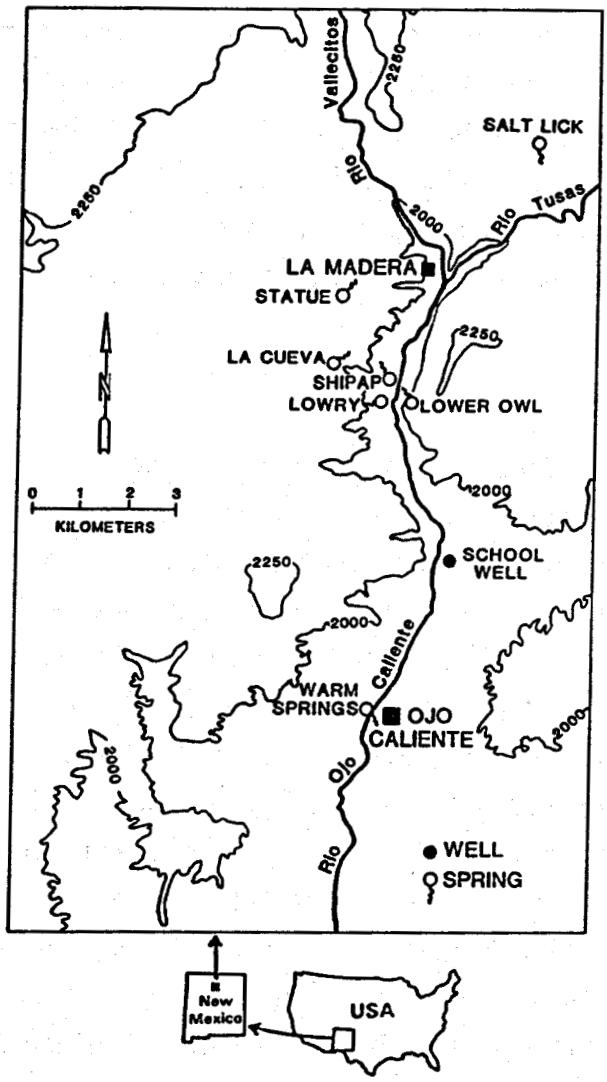

Fig. 1.
Location map of the sampling points in the Ojo Caliente-La Madera area.

impact of geothermal development on them. Recently a small paper was published with the first results obtained from this study (Stix et al. 1982).

2. GEOLOGY

Rocks in the Ojo Caliente area consist primarily of upfaulted Proterozoic crystalline rocks, unconformably overlain by Miocene basin-fill sediments that dip gently to the southeast. These Miocene rocks are, in turn, unconformably overlain by flat-lying to gently dipping Quaternary terrace gravels, sediments, travertine, and alluvium. The Precambrian sequence is upfaulted along

north-northeast-trending faults into a series of horsts so that this metamorphic sequence is exposed at the surface. The monoclinal Miocene rocks are draped over the Precambrian rocks and are cut by north to northeast-trending normal faults. The Quaternary sequence is apparently unfaulted. The reader is referred to a geologic map of the area (Fig. 2) to aid in understanding the distribution of rock units, stratigraphic relationships, and structural features.

2.1 Stratigraphy

2.1.1. Precambrian Igneous and Metamorphic Rocks.

Amphibolite, schist, and quartzite are considered the oldest rocks in the area. Amphibolite and schist are interbedded in the north-central part of the mapped area, whereas bedded Ortega Quartzite crops out in the northwest within the La Madera Mountains (Fig. 2). Younger Precambrian porphyritic rhyolite crops out west of the warm springs at Ojo Caliente. The rhyolite is phenocryst-poor to phenocryst-rich, containing crystals of quartz, microcline, and plagioclase. The rhyolite is metamorphosed, but primary relict textures such as altered glass shards have been recognized. These rocks are interpreted as hypabyssal intrusives (Cerro Colorado) and ash-flow tuffs (Treiman 1977). The youngest Precambrian rocks mapped are granite pegmatites and quartz veins, both of which are intrusive into all other Precambrian rocks. The age of this Precambrian sequence ranges from 1850 to 1700 Myr (Treiman 1977).

2.1.2. Miocene Sedimentary Rocks.

Surface exposures of Paleozoic and Mesozoic rocks do not exist in the mapped area but may subcrop adjacent to the Precambrian horsts of Cerro Colorado and the La Madera Mountains. All Tertiary rocks in the study area are Miocene in age. The most notable feature of these basin-fill deposits is the intertonguing of these formations. The Ritito Conglomerate, ranging from 1 to 120 m in thickness in the study area, consists of unsorted, poorly graded conglomerate locally derived from Precambrian rocks. Transport distance was minimal, as these are proximal deposits. The Ritito has a wide age spectrum (10 Myr?) and interfingers with the Abiquiu Tuff and Los Piños Formation.

The Abiquiu Tuff crops out in the south-central part of the study area. It is generally a grey-white, well-sorted, tuffaceous sandstone, 0- to 65-m thick with minor conglomerate and siltstone interbeds. Flows of Jarita Basalt

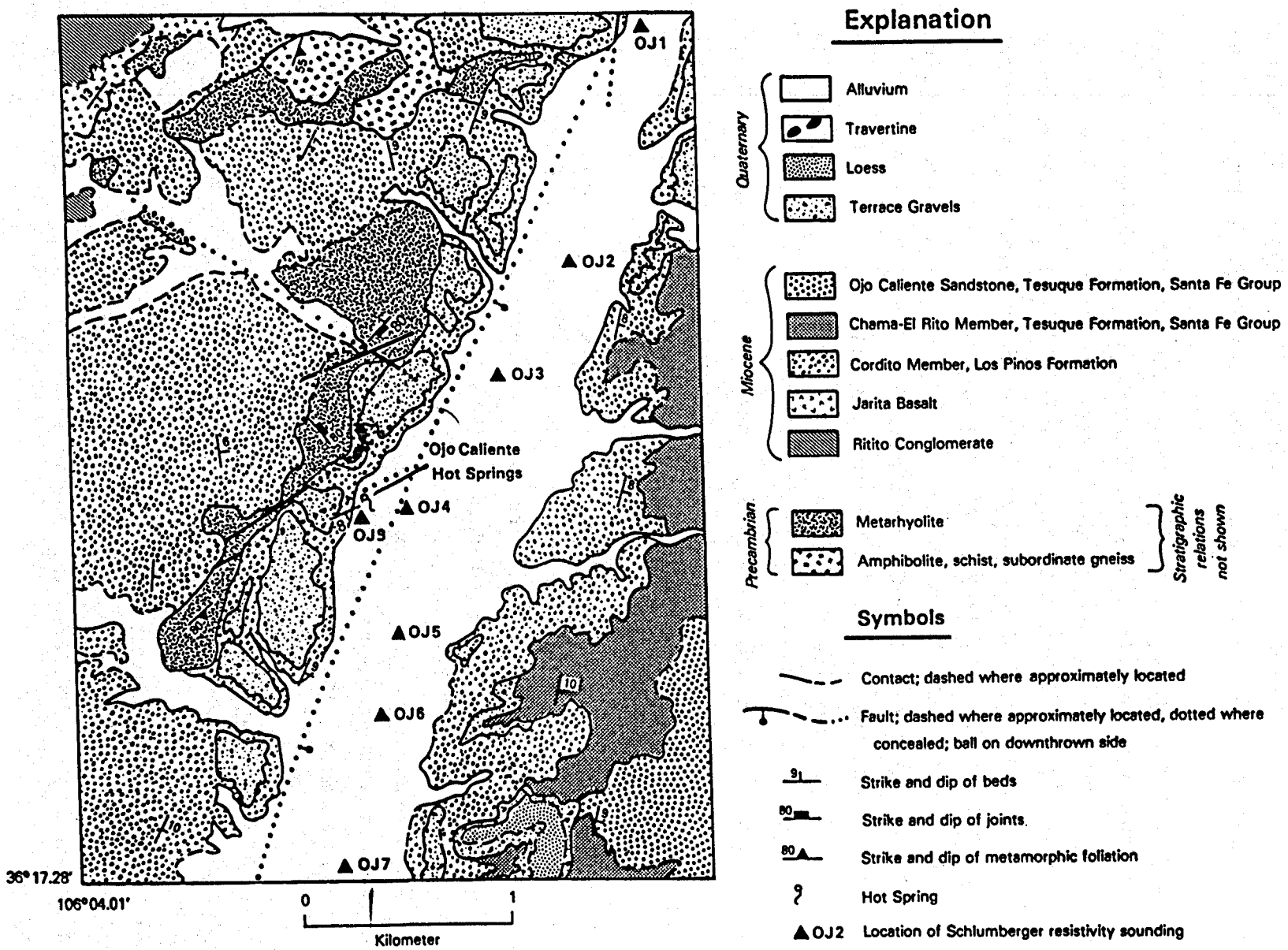

Fig. 2.
Simplified geologic map of the Ojo Caliente area (after Stix et al. 1982).

and Cerro Negro nephelinite(?) within the Abiquiu Tuff have K-Ar ages of 22.1±0.6 and 18.9±0.7 Myr, respectively (Baldridge et al. 1980). The Abiquiu Tuff intertongues with the Cordito Member of the Los Piños Formation to the north.

The Cordito Member is a 0- to 410-m-thick volcanic pebble conglomerate consisting of rhyolitic to latitic clasts. Interbeds of tuffaceous sandstone are sometimes present. In places the pebble conglomerate is well cemented by silica and/or calcite. These resistant layers have formed surfaces on which thermal and/or cold ground waters may have flowed; these layers may represent cappings for paleoaquifers. Manley (1981) suggests the Latir volcanic field to the northeast as the source of the Cordito Member. This thick wedge of volcanic detritus thins to the south and grades into the Chama-el rito Member of the Tesuque Formation, part of the Santa Fe Group, just north of Ojo Caliente (May 1979). May (1980) considers the age of the Cordito Member in the study area to range from 18 Myr to 11-12 Myr.

The Chama-el rito Member overlies and interfingers with the Los Piños Formation near Ojo Caliente. This is a well-sorted, pink-brown, generally nonvolcanic sandstone, although subordinate volcanic pebble stringers are present. It ranges from 0 to 440 m thick and grades upward into the Ojo Caliente Sandstone of the Tesuque Formation. The age of the Chama-el rito Member is uncertain but overlaps that of the Los Piños Formation. The overlying Ojo Caliente Sandstone is a brown, well-sorted quartzose sandstone that is poorly indurated and cross bedded. It is believed to be aeolian in origin; its maximum thickness is unknown. The base of the Ojo Caliente Sandstone is thought to be 11-12 Myr, and the age of the uppermost Ojo Caliente beds is thought to be as young as 5 Myr (K. Manley, U.S. Geol. Survey, personal commun., 1981).

2.1.3. Miocene Volcanics. Several basaltic units are interbedded in the sedimentary sequences described above. The Jarita Basalt has a K-Ar date of 22.1±0.6 Myr and is found in the upper part of the Abiquiu Tuff (Baldridge et al. 1980). Cerro Negro basalts, consisting of intrusive basalt, tuff breccia, and flows(?), are also associated with the Abiquiu Tuff. A Cerro Negro nephelinite flow(?) interbedded in the Abiquiu Tuff has been dated at 18.9±0.7 Myr using K-Ar methods (May 1979; Baldridge et al. 1980). Several facies of the basaltic Ojo Caliente Tuff Ring were erupted within the intertonguing

Cordito and Chama-el rito Members. The El Rito Creek vent of May (1979) is 0 to 45 m lower than the Ojo Caliente Tuff Ring facies but (1) is considered genetically related and (2) is slightly older than 13 Myr (May 1979).

2.1.4. Quaternary Sediments. Pediment gravels, terrace gravels, loess, travertine, landslide deposits, and alluvium unconformably overlie the Tertiary and Precambrian section. The pediment gravels are topographically higher and further removed from drainage basins than are the terrace gravels. The pediment deposits thus represent earlier stages of deposition and downcutting than do the river terraces.

2.1.4.1. Radiocarbon Dating. A charcoal horizon from a terrace gravel has been dated at 2800±350 years before AD 1950 using radiocarbon methods (normalized from $\sigma^{13}C$ = -20.7°/₀₀ to $\sigma^{13}C$ = -25.0°/₀₀). The surfaces of these deposits are locally flat but slope gently toward the Rio Ojo Caliente. Often several terraces at different topographic levels can be distinguished. The terrace sampled is located at latitude 36°22.086', longitude 106°03.478', approximately 2 km southwest of La Madera. The terrace is composed primarily of quartzose sandstone with subordinate silt and conglomerate interbeds. The conglomerate clasts are sub-angular to sub-rounded quartzite cobbles locally derived from exposed Ortega Quartzite. Limited paleocurrent work on imbricated conglomerates suggests a southeast direction of flow, and the terrace surface grades down to the east toward the Rio Ojo Caliente in the study area. This terrace may have been part of a fan complex with a source to the northwest.

It is unclear how this terrace correlates stratigraphically with those on the east side of the Rio Ojo Caliente. These terraces are travertine deposits up to 75 m thick. The terraces' surfaces step upward progressively from the river, indicating distinct periods of travertine deposition. The dated terrace to the west of the Rio Ojo Caliente may correlate with the lower travertine terraces. The dated terrace grades down toward the river; thus, it probably was not deposited at the same time as the topographically highest (2010 to 2040 m) travertine terraces.

The dated charcoal layer within the terrace is approximately 3 to 4 cm thick and is 1 m below the upper surface of the terrace. Numerous thin charcoal horizons outcrop beneath the dated layer; one charcoal horizon occurs 0.5 m above the dated layer but is just below a paleosol and unsuitable for

dating. In addition, a 0.5-m-thick conglomerate stringer crops out 0.5 m below the dated charcoal horizon. The proximity of the dated layer to the top of the terrace suggests that the end of terrace deposition and beginning of dissection began about 2800 years ago.

2.1.4.2. Rate of Erosion. The erosion rate can be estimated if it is assumed that (1) there have been no depositional intervals from 2800 years ago to the present, and (2) the dated charcoal horizon is in place. May (1980) has observed slope wash from higher elevations at greater distances from river drainages, causing the gentle slope of terraces toward the drainage basin. However, the dated charcoal layer is stratigraphically continuous with lower charcoal horizons and appears unaffected by slope wash.

The rate of erosion was determined by estimating a minimum relief of approximately 24 m from the top of the terrace where sampled to the bottom of the stream cut, in which the deposit is exposed, and a maximum relief of approximately 58 m from the top of the terrace where sampled to the bed of the Rio Ojo Caliente nearest the dated charcoal. Thus, a minimum rate of downcutting is 24 m every 2800 years or 0.86 cm/yr (0.76 cm/yr taking into account an error of 350 years). The maximum rate of erosion is 58 m per 2800 years or 2.07 cm/yr (2.37 cm/yr with a 350 year error). The mean rate of erosion during this period from 2800 years ago to the present day (AD 1950) was 0.76 to 2.37 cm/yr.

Baldridge et al. (1980) have estimated a rate of erosion in the Española basin of 0.0035-0.0040 cm/yr in the past 4.5 Myr and 0.0054 cm/yr in the last 3.2 Myr. They conclude the latter figure is a more accurate estimate of the present-day erosion rate. These data compare unfavorably with results presented here that show two to three orders of magnitude greater downcutting in the Holocene as opposed to Plio-Pleistocene time. The reasons for this discrepancy may be twofold: first, the rate of erosion may have increased dramatically in the Holocene as depositional rates decreased. Possibly, overgrazing by cattle has increased the erosion rate considerably in the last several hundred years (R. Gooley, Los Alamos National Laboratory, personal commun., 1983). Second, this comparison must be used with caution; the two timescales (0 to 3150 years before AD 1950 and 0-4.5 Myr) differ in time by three orders of magnitude.

2.2 Faulting: Geothermal Considerations

There is little evidence of Holocene faulting within the Tertiary and Quaternary deposits located west of the Ojo Caliente warm springs. Faulting in the Los Piños is infrequent; where it occurs, throws are not more than several meters. Several small terrace deposits of travertine indicate more extensive movement of thermal fluids in the past, but no direct geologic evidence proves Quaternary faulting. However, numerous north to northeast-trending faults are mapped in the Tertiary section in the southwest part of the study area where the Ojo Caliente fault zone terminates (May 1980). Furthermore, a major Pliocene fault, trending north-northeast and downthrown to the east, apparently runs beneath the alluvium in the Rio Ojo Caliente valley. This fault probably offsets Precambrian metarhyolite in the subsurface. Four lines of evidence point to the existence of such a fault. First, the linear alignment of a ridge of metarhyolite that lies west of Ojo Caliente trends north-northeast; the ridge may be upfaulted against buried Los Piños rocks hidden beneath the river alluvium. Second, the Ojo Caliente Fault Zone cuts Tertiary rocks 5 km southwest of Ojo Caliente and strikes north-northeast, aligned with the inferred fault in the Rio Ojo Caliente valley. Third, a fault located 8 km northeast of Ojo Caliente also follows this alignment. These structures are major faults with displacements of perhaps several hundred meters. Fourth, the location of the warm springs at Ojo Caliente appears to be controlled by the intersection of pre-Tertiary northeast-trending Precambrian shear zones with a Pliocene fault located within the valley (Fig. 2). From this evidence, the Pliocene age fault is a zone of normal faults downthrown to the east with cumulative offset of at least 100 m. This zone is possibly a reactivated Precambrian age structure.

Similarly, several lukewarm springs located south of La Madera also appear to be controlled by faulting (Figs. 1 and 2). For example, Lower Owl Spring lies along a north-northwest trending fault that offsets Ortega Quartzite, possibly against Quaternary-age travertine. La Cueva Spring emanates along a northeast-trending fault that downthrows Ojo Caliente sandstone to the northwest relative to older Los Piños gravels. The effect of faulting upon Lowry and Shipap Springs is difficult to evaluate, as terrace gravels and alluvium conceal the structure.

3. HYDROLOGIC SETTING

The Ojo Caliente thermal area is located in the northern Española basin, which is part of the Rio Grande rift. This explains why the drainage basin of the Rio Ojo Caliente (Rio Vallecitos and Rio Tusas to the north of La Madera) has a north-south extension (Fig. 1). The Rio Ojo Caliente is a tributary of the Rio Chama, itself flowing into the Rio Grande, a major stream stretching from Colorado to Texas, through New Mexico. The Rio Ojo Caliente, which is a perennial stream, flows on the west side of the valley about 250 m east of the warm springs. The stream bed is composed of Quaternary gravels, sands, and silts, whereas the warm springs emergence zone is located at the boundary between the Quaternary valley fill and Precambrian metarhyolite (see Fig. 2 for exact geologic relationships).

At Ojo Caliente Resort, five warm springs have been tapped to supply water to the bathhouses, while four shallow wells have been drilled in the valley fill for domestic water supply (Fig. 3). Three of the wells tap a mixture of mineralized warm water and cold dilute water in the shallow aquifer. The fourth one, the "Hot well," strikes the warmest water known in

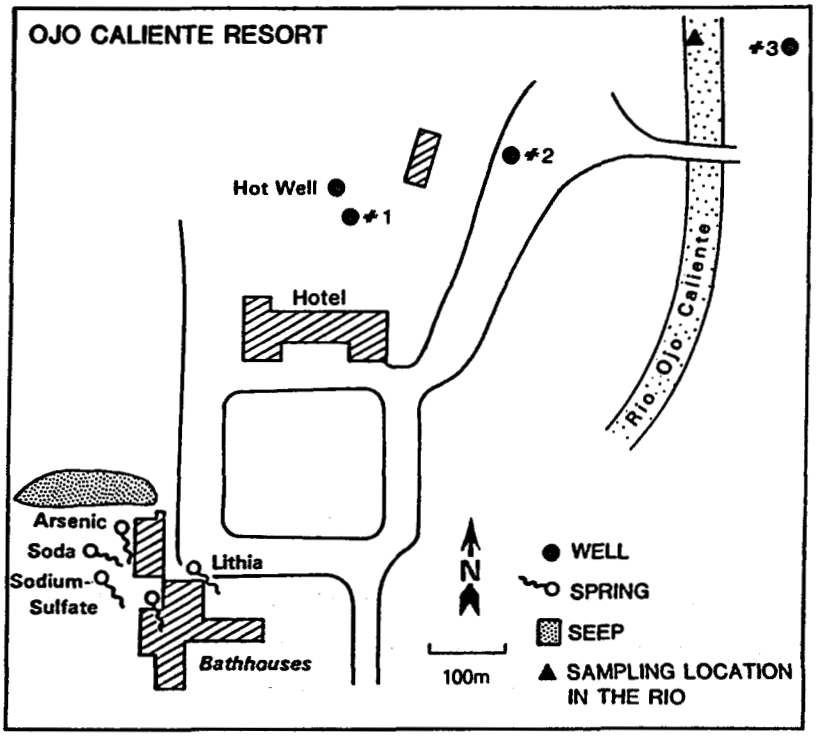

Fig. 3.
Location map of the sampling points at Ojo Caliente Resort.

the area (54°C) but has been unused since its drilling in 1951-52 (Summers 1976). Its rather constant water level (0.7±0.1 m below ground surface) indicates a constant pressure of upwelling thermal water in absence of any pumping, and it can be called a nonflowing artesian well.

Between Ojo Caliente and La Madera, a shallow well taps cold water in the Quaternary aquifer to supply the Mesa Vista school. Slightly south of La Madera, there occurs a group of lukewarm springs in the middle and both sides of the Rio Ojo Caliente valley. One isolated cold spring (Salt Lick) issues north of La Madera that displays unique characteristics (Fig. 1). The emergence elevations for all these sampling points range from 1900 m for the spa area to 2100 m for Salt Lick spring. If one considers the drainage basin upstream from Ojo Caliente, which stretches all the way north to Colorado, the highest elevation point is 3330 m (San Antonio Mountain) while the lowest point is the Rio Ojo Caliente at the spa (1895 m). Estimation of the total elevation range of the basin using a 1:250 000 topographic map indicates that about 70% of the total basin is between 2400 and 3000 m, and that the average topographic elevation of the basin is 2650 m. Five kilometers north of Ojo Caliente Resort and 120 m upstream from the bridge on State Highway 96, a gauge records the water level of the Rio Ojo Caliente. The elevation of the gauge is 1938 m and the drainage area is 1085 km^2 (U.S. Geological Survey 1981). Records of the discharge of the Rio Ojo Caliente have been taken from April 1932 to the current year. The average annual discharge for a period of 48 years (1932-1980) is 1.914 m^3/s, while the extreme recorded values are 88.9 m^3/s (April 21, 1958) and 0.006 m^3/s (August 17, 1956).

4. GEOCHEMICAL CHARACTERISTICS OF THE WATERS

4.1 Field and Laboratory Procedures

Samples from 1979 to 1981 were collected according to the methods described in Goff et al. (1982); temperature was recorded with mercury thermometers; field pH was determined using an analog pH meter (Porto-Matic 175, Instrumentation Laboratory, Inc.); field Eh was measured by standardizing the pH meter with Quinhydrone (Kodak 217) mixed in pH4 and pH9 buffer solutions; conductivity was recorded in the laboratory and discharge estimated visually. Since 1982, a multiparameter digital device (Portalab 500, Presto-Tek Corp.) takes care of temperature, pH, Eh, and conductivity. Discharge has been measured with graduated buckets.

Samples of water for analysis were filtered when necessary, using a vacuum pump system with a 0.45-μm filter paper. The following types of samples were collected for analyses in various polyethylene or glass bottles with Polyseal caps: (1) a 500-mℓ plastic bottle of raw water for anions; (2) a 250-mℓ plastic bottle of filtered and acidified water for cations and trace elements; (3) a 125-mℓ plastic bottle of filtered water diluted to 1:10 with deionized water for silica; (4) a 500-mℓ glass bottle of raw water for tritium; and (5) a 125-mℓ glass bottle of raw water for oxygen-18 and deuterium. Acidification was done by adding concentrated HNO_3 until the pH dropped lower than 2. The chemistry was analyzed entirely by the Fenton Hill laboratory (Los Alamos National Laboratory), and the analytical methods are given in Goff et al. (1982). Oxygen-18 and deuterium analyses were provided by the Bureau des Isotopes Stables, Centre d'Etudes Nucléaires, Saclay, France, whereas the tritium data were obtained from Teledyne Isotopes, Westwood, New Jersey.

4.2 Physical Parameters

4.2.1. Temperature. Very few temperature data are available for the Rio Ojo Caliente and the shallow cold ground water; therefore, they do not allow calculation of precise yearly averages. The group of springs around La Madera display temperatures between 15 and 29°C, values which are higher than the shallow cold ground-water temperature (Table I). For example, the shallow School well 3.5 km north of the spa, without apparent thermal water contamination, has a temperature of 13°C; this value is likely to be in the range of variation of the mean shallow ground-water temperature for the area. Usually, cold ground waters display temperatures 1 to 1.5°C above the mean yearly air temperature (Walton 1970). Knowing the average air temperatures and elevations for Taos, Los Alamos, and Santa Fe, respectively 8.4, 9.0, and 9.7°C, a value for Ojo Caliente can be roughly estimated at 10 to 11°C (Weather Bureau, Albuquerque and Environmental Surveillance, Los Alamos National Laboratory, oral communications, 1983). Ground-water temperature is then deduced to be in the range of 11 to 13°C.

Temperature measurements have been taken several times in the Rio Ojo Caliente upstream from the spa: strong variations occur according to the time of day and the season. Although a range of 8 to 19°C was observed, these are not thought to represent the extreme values.

TABLE I

PHYSICAL PARAMETERS FOR THE WATERS OF OJO CALIENTE AREA[a]

Name	No.	Date	Temperature (°C)	pH	Eh (mV)	Conduct. (μS/cm)	Discharge (ℓ/min)	Reference[b]
Rio Ojo Caliente	OC-19	4/82	7.7	8.29		206		
School well[c]	OC-27	6/82	13.4	7.52	136	978	>55	
Well #2	-	4/65		7.8		1050		1
Statue spring	OC-26	6/82	29.2	6.26	150	1660	110	
Shipap spring	OC-9	7/80	27.5	6.01	210	1790		
Lower Owl spring	OC-11	11/81	28	6.20	190	1750	80	
Lower Owl springs[d]	OC-8	7/80	23	6.46	200	1710	60	
La Cueva spring	OC-7	7/80	17	6.13	160	1760	15[e]	
Lowry spring	OC-23	4/82	25.0	6.31		1850		
Lowry spring	OC-12	11/81	25	6.15	180	1820	60	
Salt Lick spring	-	7/76		8.2				2
Salt Lick spring	OC-10	11/81	14.5	7.60	140	1130	4	
Well #2[c]	OC-21	4/82	14.7	7.39		1880		
Well #1	-	4/65		7.8		2380		1
Tap water[f]	OC-6	7/80	25			2900		
Well #1[c]	OC-20	4/82	34.3	6.88		3000		
Lithia spring	OC-2	12/79	38	6.55		3900		
Lithia spring	OC-13	4/82	41.9	7.08		4190		
Iron spring	OC-1	12/79	43	6.40		4100	40	
Soda spring	-	1891-93						1
Soda spring	-	10/47	35.0			3890		1
Arsenic spring	OC-5	7/80	43.5	6.60	180	4000	20	
Sodium Sulfate spring	OC-3	12/79	40	6.20		4100	15	
Iron spring	-	12/74	42.8	6.65				1
Sodium Sulfate spring	OC-16	4/82	41.3	7.02		4250	45	
Arsenic spring	-	10/49	45.0	7.1		3900		1
Sodium Sulfate spring	-	10/49	40.6	6.9		3920		1
Arsenic spring	OC-14	4/82	38.3	7.44		4200		
Iron spring	OC-15	4/82	42.2	7.26		4250		
Soda spring	OC-17	4/82	27.3	6.86		4220		
Soda spring	-	10/49		7.2		3910		1
Hot well[g]	OC-4	12/79	54	6.75		3900	0	
Arsenic spring	-	12/74	38.3	7.1		3800		1,2
Sodium Sulfate spring	-	10/47	32.2			3890		1
Iron spring	-	11/65		9.09		3300		1
Hot well[h]	OC-25	6/82	54.2	7.14	88	4440	0	
Hot well[i]	OC-18	4/82	53.6	7.98		4560	0	
Well #3[h]	OC-28	6/82	12.1	7.03	-125	4110	0	
Iron spring	-	12/74	42.8	6.6		3900		1,2

[a] All measurements from the years 1979 to 1982 were made in the field by the Los Alamos National Laboratory.
[b] The sample arrangement is the same for Tables I and III to VII and is explained in Table III, note a.
1 = Summers, 1976; 2 = Trainer and Lyford, 1979
[c] These two references are still valid for Tables III, IV, and VI.
[d] Wellhead sampling during pumping.
[e] The sample OC-8 is a mixture of two springs of the same type emerging above. OC-11 is one of them.
[f] Total flow of all surrounding emergences equals 60 ℓ/min.
[g] Mixture of water pumped in a tank from wells #1 and #2 and used as potable water supply.
[h] Sampling and temperature measurement at the top of water column (about 1 m below ground level).
[i] Sampling at the bottom of the well and temperature measured at 10 m below ground level.
Sampling at the top of water column and temperature measured at 10 m below ground level.

Temperature logs are available from two wells (Hot well and well #3) at the spa, drilled in the shallow aquifer for potable water supply (Fig. 3). Both tap the thermal water, although neither is used. An initial temperature log was made in 1952, probably after completion of the well (Fig. 4). From the drilling report, the hot water is said to have been encountered at a depth of 26.5 m, whereas at 15 m the water was still cold (Summers 1976). Calculation of a temperature gradient is not sensible because the temperature distribution of this system is purely convective. This 31-year-old temperature log has been duplicated by a recent one (J. Hunter, 1981, Los Alamos

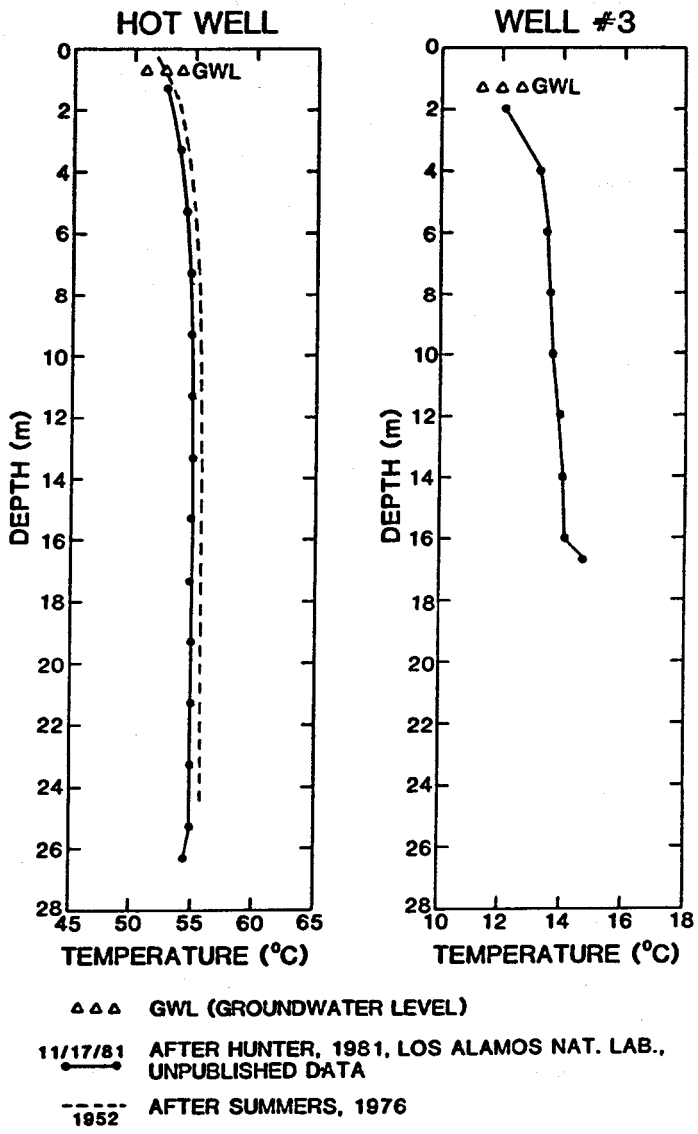

Fig. 4.
Temperature logs for the Hot well and well #3 at Ojo Caliente Resort. The two logs carried out in the Hot well are very similar despite 30 years between the two measurements.

National Laboratory, unpublished data), which has a very similar curve, about 0.7°C colder than in 1952 (Fig. 4). The recent temperature log of well #3 shows a steady increase of temperature with depth, with a maximum temperature of 14.8°C. This value is probably too high for a shallow cold aquifer, unless it is the unmixed summer water percolating laterally from the river into the Quaternary aquifer. In addition, the conductivity of well #3 is very high (4110 µS/cm), almost reaching the value of the thermal water (4200-4500 µS/cm), indicating that thermal water spreads into the sand and gravel of the shallow aquifer and is cooled by the proximity of the river (~100 m).

At Ojo Caliente, temperature of the warm water has been measured for more than a century. Loew in 1875 described four warm springs with temperatures ranging from 42 to 46°C; several authors, from 1875 to 1974, indicated values from 32 to 50°C for three to five warm springs (Summers 1976; Table II). These values are very close to the ones recorded currently, even if it is not possible to evaluate the precision of past measurements. On the other hand, the way in which the springs are now trapped is surely different from one century ago. Also, none of the recent temperatures have been measured where water flows directly from the fissures but rather from concrete pipes and tanks. These facts explain why 50°C is not encountered anymore in the springs. However, the water at the top of the unused Hot well (0.7 m below ground level) reaches 53°C.

4.2.2. pH and Eh. Natural waters of this study display a small range of pH variations from 6 to 8.3, but each type of water has specific values. Surface waters, here represented by the Rio Ojo Caliente, have a slightly basic pH of 8.3, possibly a result of man-made pollution. The ground water influenced by river percolation and tapped by the shallow wells shows a variable pH from 6.9 to 7.8. A very stable pH from 6.0 to 6.5 is measured at the group of La Madera springs. Finally, the thermomineral water of Ojo Caliente, due to degassing and temperature drop at emergence, has a more or less neutral pH of 7±0.5 varying with time and sampling locations.

Only a few Eh values are available, and all but one are in the narrow range of 90 to 210 mV, showing weak oxidizing conditions. A sole negative Eh value of -125 mV for the well #3 reflects slight reducing conditions, confirmed by black suspension in the water, likely to be reduced iron.

TABLE II

SELECTED HISTORIC DATA OF THE WARM SPRINGS OF OJO CALIENTE COMPARED WITH RECENT DATA[a]

Sampling date	Temperature (°C)	TDS (mg/ℓ)	Total discharge (ℓ/min)	Reference[b]
-	42-46	2540-2600	-	Loew (1875)
-	47-49	-	-	Cope (1875)
-	42-50	-	230	Peale (1886)
1891-93	-	3660	-	Clark (1893)
-	32-50	2320	260	Crook (1899)
-	32-50	-	790	Jones (1904)
-	37-45	-	1320	Stearns et al. (1937)
10/1949	41-45	3630-3720	-	USGS
12/1965	43	3140	370	Summers (1976)
12/1974	38-43	3580-3670	-	USGS
4/1982	27-44	3630-3670	340	this report

[a] All values of temperature, total dissolved solids (TDS), and total discharge are rounded off to the nearest 1°C, 10 mg/ℓ, and 10 ℓ/min, respectively.

[b] All references before this report were taken from Summers (1976).

4.2.3. Conductivity. Conductivity is a quick and handy field tool for evaluation of spring and aquifer systems. Unfortunately, field measurements of conductivity only began in 1982 for this study. Previous values were recorded at the laboratory, causing roughly a 10% decrease and making comparisons difficult. In spite of this problem, marked groups of conductivity can be deciphered. Surface water is the least conductive with 200 µS/cm, uncontaminated ground waters reach nearly 1000 µS/cm, and mixtures of cold and thermal ground waters range from 1000 to 3000 µS/cm. The spring group of La Madera is very stable around 1750 µS/cm, while Ojo Caliente thermomineral water tops with 4000±200 µS/cm.

4.2.4. Discharge. Flow rate is usually the poorest of the field parameters, because of the bad quality and the small number of measurements. Unfortunately this study does not break the tradition. Discharge was correctly measured only at a very few sampling locations.

La Madera springs have discharge values ranging from 15 to 80 ℓ/min. At Ojo Caliente Resort, a total discharge of 340 ℓ/min for the five warm springs was measured in two drainage ditches. Each spring should have its own unique discharge, and values of 15 to 45 ℓ/min were recorded on three different emergences. Amazingly, five historical values of total discharge are available, varying from 230 to 1320 ℓ/min (Table II). Again, it is impossible to assess the validity of such numbers without knowledge of the measurement conditions.

4.3 Chemical Parameters

All the chemistry is listed in Tables III and IV respectively for the major, minor, and trace elements.

4.3.1. Chemical Classification and Major Constituents. Several types of water can be distinguished by means of a chemical classification based on the major ions. A chemical formula is developed with the ions whose concentration reaches more than 10% of the Total Dissolved Ions (TDI), expressed in meq/ℓ. Only three cations (Na, Ca, Mg) and three anions (HCO_3, SO_4, Cl) are represented, as observed in most other circumstances (Vuataz 1982). Sometimes these six ions account each for more than 10% of the TDI, and sometimes only two form the chemical formula (Table V). The thermomineral water of Ojo Caliente contains Na and HCO_3 for a total of 45 and 40% of the TDI, respectively.

Sodium-bicarbonate thermal waters are common in granitic or rhyolitic type of rocks and are encountered in many thermal provinces, such as the French Massif Central. For example, the thermomineral springs of Chateauneuf-les-Bains have very similar characteristics compared with Ojo Caliente (Fouillac et al. 1976). The same chemical formula is also encountered for the shallow ground water containing a high percentage of thermal water, such as well #1 and the tap water. With a decreasing proportion of the mineralized thermal water, the formula changes and includes the other ions (well #2). The only type of water that does not have Na as first cation is the surface water

TABLE III

MAJOR AND MINOR CHEMICAL PARAMETERS (mg/ℓ) AND IONIC BALANCE (meq/ℓ) FOR THE WATERS OF OJO CALIENTE AREA[a]

Name	No.	Date	Na^+	K^+	Ca^{++}	Mg^{++}	Li^+	Sr^{++}	HCO_3^-	Cl^-	SO_4^{--}	F^-	Br^-	SiO_2	B	TDS[b]	Σcations[c]	Σanions[c]
Rio Ojo Caliente	OC-19	4/82	12.1	1.0	22.4	5.4	0.02	0.17	88	11.9	21.0	0.77	<0.05	22	0.03	185	2.12	2.26
School well	OC-27	6/82	110	5.4	74	24	0.22	1.01	412	45.5	124	0.82	0.08	36	0.22	833	10.64	10.66
Well #2	-	4/65	102	4.7	80	29			274	83	158	0.55					10.93	10.15
Statue spring	OC-26	6/82	160	15	126	48	0.41	1.15	649	108	254	1.44	<0.05	23	0.41	1386	17.66	19.05
Shipap spring	OC-9	7/80	172	15	139	57	0.01	0.80	678	114	262	1.6	<0.5	21	0.5	1461	19.51	19.87
Lower Owl spring	OC-11	11/81	179	14	145	58	0.5	1.02	671	114	273	1.3	0.37	21	0.55	1479	20.24	19.97
Lower Owl springs	OC-8	7/80	176	15	128	58	0.03	0.88	609	116	274	1.6	<0.5	21	0.5	1401	19.22	19.05
La Cueva spring	OC-7	7/80	172	13	148	53	0.01	1.20	673	116	266	1.3	<0.5	34	0.5	1479	19.59	19.91
Lowry spring	OC-23	4/82	180	14	150	60.1	0.52	1.23	716	119	278	1.23	0.37	17	0.52	1538	20.72	20.95
Lowry spring	OC-12	11/81	189	14	152	60	0.6	0.96	693	121	286	1.3	0.62	20	0.58	1539	21.21	20.80
Salt Lick spring	-	7/76	225	4.7	14	1.1			310	125	96	10		32	0.4	818	10.70	11.13
Salt Lick spring	OC-10	11/81	232	3.6	15	1.1	1.0	0.25	305	127	93	11.8	0.75	31	0.45	822	11.17	11.15
Well #2	OC-21	4/82	280	6	110	32.5	0.86	1.13	752	132	190	2.3	0.34	34	0.45	1542	20.64	20.13
Well #1	-	4/65	496	16	40	16			907	149	155	7.5					25.30	22.69
Tap water	OC-6	7/80	580	18	65	19.2	2.4	0.84	1350	183	184	14.9	<0.5	50	1.0	2469	30.88	31.91
Well #1	OC-20	4/82	620	18	70	21.6	2.04	1.34	1410	190	193	8.4	0.83	50	0.91	2586	33.03	32.94
Lithia spring	OC-2	12/79	867	28.5	23.6	8.70	2.7	1.16	2070	227	173	13.5		58.5	1.47	3475	40.75	44.64
Lithia spring	OC-13	4/82	950	30	26	9.5	3.57	1.48	2160	227	151	11.8	1.02	57	1.40	3630	44.72	45.58
Iron spring	OC-1	12/79	953	29.0	21.0	6.60	2.2	1.14	2090	229	171	14.2		58.9	1.53	3578	44.13	45.02
Soda spring	-	1891-93	996	31.4	22.8	9.5	3.4		2150	231	151	5.2	0	60.2	0.29	3661	46.54	45.17
Soda spring	-	10/47			28	8.7			2200	232	168	16		60				
Arsenic spring	OC-5	7/80	914	31	22	7.8	0.38	1.22	1690	235	150	16.1	<0.5	61	1.6	3131	42.37	38.30
Sodium Sulfate spring	OC-3	12/79	866	31.3	20.6	6.60	2.4	1.04	2100	237	187	15.5		64.3	1.50	3533	40.41	45.81
Iron spring	-	12/74	980	31.5	29	8.5	4.3		2070	237	149	13.5	0.66	55	1.0	3579	46.20	44.43
Sodium Sulfate spring	OC-16	4/82	950	28	20	7.1	3.64	1.49	2150	237	153	14.0	1.12	61	1.41	3628	44.18	45.86
Arsenic spring	-	10/49	928	30	25	8.9			2160	238	156	16		63	1.6	3627	43.11	46.20
Sodium Sulfate spring	-	10/49	933	34	24	7.6			2160	238	156	16		63	1.7	3633	43.28	46.20
Arsenic spring	OC-14	4/82	950	30	22	8.1	3.59	1.49	2180	238	157	13.1	0.93	59	1.40	3665	44.40	46.41
Iron spring	OC-15	4/82	950	30	22	8.1	3.38	1.45	2190	238	154	14.1	1.02	61	1.42	3674	44.37	46.56
Soda spring	OC-17	4/82	950	28	20	7.0	3.50	1.44	2190	240	154	14.4	1.14	62	1.39	3673	44.15	46.64
Soda spring	-	10/49	997	29	25	9.0			2180	240	162	16		66		3724	46.10	46.71

TABLE III (cont)

Name	No.	Date	Na^+	K^+	Ca^{++}	Mg^{++}	Li^+	Sr^{++}	HCO_3^-	Cl^-	SO_4^{--}	F^-	Br^-	SiO_2	B	TDS[b]	Σcations[c]	Σanions[c]
Hot well	OC-4	12/79	927	27.8	7.3	2.90	5.5	0.48	1870	242	195	20.8		43.4	1.54	3344	42.44	42.63
Arsenic spring	-	12/74	1000	30.6	28	7.8	4.3		2140	242	149	12.8	0.15	56	1.37	3672	46.94	45.67
Sodium Sulfate spring	-	10/47			28	8.7			2210	245	165	16		56	0.32			
Iron spring	-	11/65	993	36	6	7.7	2.7		1640	246	132	3.0		71	1.1	3139	45.44	36.72
Hot well	OC-25	6/82	940	30	17	5.4	3.17	1.28	2130	246	160	17.3	1.22	65	1.41	3618	43.43	46.10
Hot well	OC-18	4/82	1000	28	8	3.9	3.64	0.65	2190	253	164	17.9	1.01	52	1.46	3724	45.47	47.40
Well #3	OC-28	6/82	880	20	38	3.6	3.14	2.01	2220	256	66.5	13.1	7.20	48	1.46	3559	41.48	45.77
Iron spring	-	12/74	890				3.3		2070	270			1.4	63	1.5			

[a] The water sources and the samples are arranged by increasing Cl concentration. In case of similar Cl content, TDS is prevalent. The ion sequence is made by decreasing concentration of cations and anions, respectively, as observed in the most mineralized samples. The same sample arrangement is made in Tables I and III to VII.

[b] TDS (Total Dissolved Solids): sum of the chemical species listed in this table.

[c] Sum of the cations and sum of the anions in milliequivalent per liter (meq/ℓ) used to check the ionic balance.

TABLE IV

TRACE ELEMENTS (mg/ℓ) FOR THE WATERS OF OJO CALIENTE AREA[a]

Name	No.	Date	Ag	Al	Ba	Cd	Co	Cr	Cu	Fe	Mn	Mo	NH_4	Ni	NO_3	Pb	PO_4	Zn
Rio Ojo Caliente	OC-19	4/82	<0.01	0.68	0.06	<0.01	<0.01	<0.01	0.01	0.44	0.02	<0.01	<0.01	<0.01	<0.05	<0.01	<0.05	0.02
School well	OC-27	6/82	<0.01	0.11	0.11	<0.01	<0.01	<0.01	<0.01	0.01	<0.01	<0.01	0.03	<0.01	0.97	0.05	<0.2	0.04
Well #2	-	4/65								0.38	0.12				0			
Statue spring	OC-26	6/82	<0.01	0.10	0.04	<0.01	<0.01	<0.01	<0.01	0.03	<0.01	<0.01	0.01	<0.01	1.99	0.02	<0.2	0.44
Shipap spring	OC-9	7/80	<0.001	<0.001[b]	0.026	<0.001	<0.001	0.002	0.008	0.008	0.006	<0.002		0.006	<0.5	<0.004	<0.5	0.034
Lower Owl spring	OC-11	11/81	<0.001	<0.01	0.008	<0.001	<0.001	<0.001	0.002	0.020	<0.01	<0.01	0.04	0.007	<0.1	<0.1	<0.1	0.02
Lower Owl springs	OC-8	7/80	<0.001	0.160[b]	0.025	<0.001	<0.001	0.001	0.008	0.024	<0.001	<0.002		0.010	<0.5	<0.004	<0.5	0.008
La Cueva spring	OC-7	7/80	<0.001	1.00?[b]	0.010	<0.001	<0.001	0.002	<0.001	0.020	0.002	<0.002		<0.002	<0.5	<0.004	<0.5	0.030
Lowry spring	OC-23	4/82	<0.01	0.09	0.03	<0.01	<0.01	<0.01	0.01	0.01	<0.01	<0.01	<0.01	<0.01	<0.05	0.05	<0.05	0.05
Lowry spring	OC-12	11/81	<0.001	<0.01	0.008	<0.001	<0.001	<0.001	0.003	0.024	<0.01	0.09	0.05	0.007	0.7	<0.1	<0.1	<0.01
Salt Lick spring	-	7/76																
Salt Lick spring	OC-10	11/81	<0.001	<0.01	0.010	<0.001	<0.001	<0.001	<0.001	0.010	<0.01	0.08	0.04	0.002	<0.1	<0.1	<0.1	<0.01
Well #2	OC-21	4/82	<0.01	0.02	0.19	<0.01	0.01	<0.01	0.01	1.04	0.54	<0.01	<0.01	<0.01	<0.05	0.03	<0.05	0.04
Well #1	-	4/65								0.31	0				0			
Tap water	OC-6	7/80	<0.001		0.184	<0.001	<0.001	0.001	0.032	0.012	0.100	0.005		<0.002	<0.5	0.004	<0.5	0.070
Well #1	OC-20	4/82	<0.01	0.11	0.17	<0.01	0.02	<0.01	<0.01	0.08	0.25	<0.01	<0.01	<0.01	<0.05	<0.01	<0.05	0.03
Lithia spring	OC-2	12/79	0.001	0.015[b]	0.097	0.013	0.001	<0.001	0.002	0.020	0.035	0.007		<0.001		<0.01		0.002
Lithia spring	OC-13	4/82	<0.01	<0.01	0.10	<0.01	0.03	<0.01	<0.01	0.13	0.03	<0.01	0.13	<0.01	<0.05	<0.01	<0.05	<0.01
Iron spring	OC-1	12/79	0.001	0.017[b]	0.101	0.013	0.001	<0.001	<0.001	0.400	0.030	0.008		<0.001		<0.01		<0.001
Soda spring	-	1891-93		0.18						0.56	0				traces		0.2	
Soda spring	-	10/47													1.7			
Arsenic spring	OC-5	7/80	<0.001	0.28?[b]	0.144	0.002	<0.001	<0.001	0.008	0.050	0.031	0.005		<0.002	<0.5	0.024	<0.5	0.024
Sodium Sulfate spring	OC-3	12/79	0.001		0.097	0.012	<0.001	<0.001	0.003	0	0.028	0.002		0.001		<0.01		0.002
Iron spring	-	12/74		0.03						0.06	0.15				0.12			
Sodium Sulfate spring	OC-16	4/82	<0.01	<0.01	0.11	<0.01	0.01	<0.01	<0.01	0.23	0.03	<0.01	0.01	<0.01	<0.05	0.01	<0.05	<0.01
Arsenic spring	-	10/49								0.01					0.8			
Sodium Sulfate spring	-	10/49								0.02					0.5			
Arsenic spring	OC-14	4/82	<0.01	<0.01	0.11	<0.01	0.01	<0.01	0.01	0.04	0.01	<0.01	0.08	<0.01	<0.05	<0.01	<0.05	<0.01
Iron spring	OC-15	4/82	<0.01	<0.01	0.11	<0.01	<0.01	<0.01	<0.01	0.04	0.03	<0.01	0.04	<0.01	<0.05	0.03	<0.05	<0.01
Soda spring	OC-17	4/82	<0.01	0.03	0.12	<0.01	0.02	<0.01	0.01	0.04	0.06	<0.01	<0.01	<0.01	<0.05	<0.01	<0.05	0.02
Soda spring	-	10/49													0.9			

TABLE IV (cont)

Name	No.	Date	Ag	Al	Ba	Cd	Co	Cr	Cu	Fe	Mn	Mo	NH_4	Ni	NO_3	Pb	PO_4	Zn
Hot well	OC-4	12/79	0.001	0.015[b]	0.061	0.009	0.001	<0.001	0.002	0.002	0.014	0.005		<0.001		<0.01		0.001
Arsenic spring	-	12/74		0.02						0.06	0.15				0.11			
Sodium Sulfate spring	-	10/47													1.7			
Iron spring	-	11/65								0.57	0.15						0.6	
Hot well	OC-25	6/82	<0.01	0.14	0.13	<0.01	0.03	<0.01	<0.01	0.22	0.02	<0.01	0.10	0.80	<0.05	0.05	<0.1	0.15
Hot well	OC-18	4/82	<0.01	0.08	0.05	<0.01	0.01	<0.01	<0.01	0.06	0.02	<0.01	<0.01	<0.01	<0.05	0.03	<0.05	0.04
Well #3	OC-28	6/82	<0.01	0.18	0.156	<0.01	<0.01	<0.01	<0.01	35	0.13	<0.01	0.03	0.10	<0.05	0.02	<0.2	0.04
Iron spring	-	12/74																

[a] The sample arrangement is the same for Tables I and III to VII and is explained in Table III, note a. The chemical parameter sequence is made by alphabetical order.

[b] These Al^{+++} values correspond to the ionized aluminum (filtration and extraction in the field), while the other Al results represent the total aluminum (filtration and acidification only).

TABLE V

CHEMICAL CLASSIFICATION OF THE WATERS FROM OJO CALIENTE AREA[a]

Water types	Classification[b]
Rio Ojo Caliente	Ca>Na>Mg; HCO_3>>SO_4
School well	Na>Ca; HCO_3>>SO_4
Statue spring	Na>Ca>Mg; HCO_3>>SO_4
Shipap spring	"
Lower Owl springs	Na>Ca>Mg; HCO_3>SO_4
La Cueva spring	"
Lowry spring	Na>Ca>Mg; HCO_3>>SO_4
Salt Lick spring	Na; HCO_3>Cl
Well #2 (1965)	Na>Ca>Mg; HCO_3>SO_4>Cl
Well #2 (1982)[c]	Na>>Ca>>Mg; HCO_3>>SO_4>Cl
Tap water	Na; HCO_3
Well #1	
5 warm springs	
Hot well	
Well #3	

[a] The sample arrangement is the same for Tables I and III to VII and is explained in Table III, note a.

[b] In the chemical formula, the ion sequence is made by decreasing concentration of cations and anions, respectively. Reported concentrations in meq/ℓ are higher than 10% of the sum of the ions in meq/ℓ (= Total Dissolved Ions or TDI). The symbol >> means that the concentration in meq/ℓ of the ion on the left is equal or greater to the double of the concentration of the ion on the right.

[c] In the 1982 sample, the water collected from well #2 contained much more thermal water than in the 1965 sample. Therefore the chemical formula is slightly modified, tending towards the thermal water formula.

(Rio Ojo Caliente); even the so-called dilute shallow ground water (School well) is essentially a sodium-bicarbonate water. This feature, linked with a rather high silica concentration, suggests that the valley alluvium aquifer is mainly composed of fragments of granitic and metamorphic rocks.

The group of La Madera springs also has Na and HCO_3 as principal ions, but Ca, Mg, Cl, and SO_4 are much more important in comparison with the Ojo Caliente thermal water.

Graphically, the bulk chemical composition can be compared between several groups of waters by means of ionic composition diagrams [Figs. 5(a) and 5(b)]. On Fig. 5(a), a concentration-dilution chemical pattern is observed between the two springs of La Madera group (Lowry and Statue), the shallow ground water (School well), and the surface water (Rio Ojo Caliente). These four samples seem to be related either hydrologically (mixing) or geologically (same mineralization origin). Only Salt Lick spring, north of La Madera, is unlikely to have any relation with the previous described waters.

On the second ionic composition diagram [Fig. 5(b)], the Ojo Caliente thermal water system is shown with the School well and the Rio Ojo Caliente, again for comparison with shallow dilute ground and surface waters. The same concentration-dilution chemical pattern is seen between the most and the least mineralized waters, but only for half of the ions (Na, HCO_3, Cl, and F). The other half, namely Mg, K, Ca, and SO_4, does not behave the same way, because some ions such as Mg and Ca are more concentrated in the dilute shallow ground water (School well) than in the mineralized thermal water (Iron spring). Wells #1 and #2 appear they are the result of a mixture between the two latter types of water.

The five thermal springs of Ojo Caliente all have been named with a chemical characteristic, namely Lithia, Soda, Iron, Arsenic, and Sodium Sulfate springs (Table III). These springs were checked to see if their names are justified by showing anomalous concentrations of Li, HCO_3, Fe, As, and Na-SO_4, respectively. None of the springs have a concentration of its supposedly specific parameter higher than one standard deviation from the average, and in essence they are all the same. Arsenic analyses are not available and therefore could not be checked. However, one can presume that the five thermal springs of the resort were named a long time ago on the basis of one single analysis.

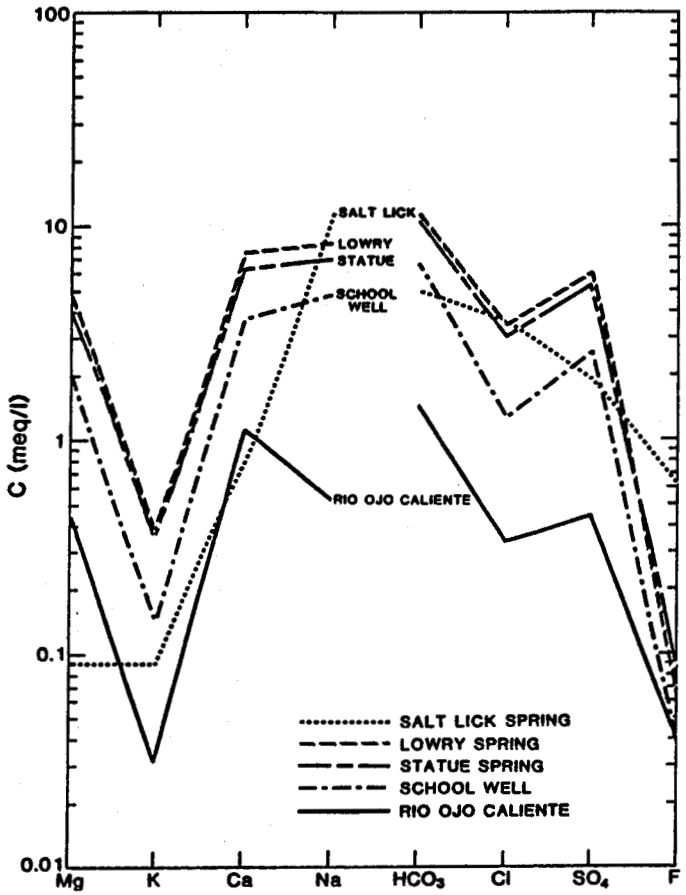

Fig. 5(a).
Ionic composition diagram of the different types of water around La Madera. The springs located south of La Madera display the same type of chemistry, whereas Salt Lick spring has a more alkaline composition. The Rio Ojo Caliente and the School well represent the dilute surface water and the uncontaminated shallow aquifer before possible mixing with thermal water.

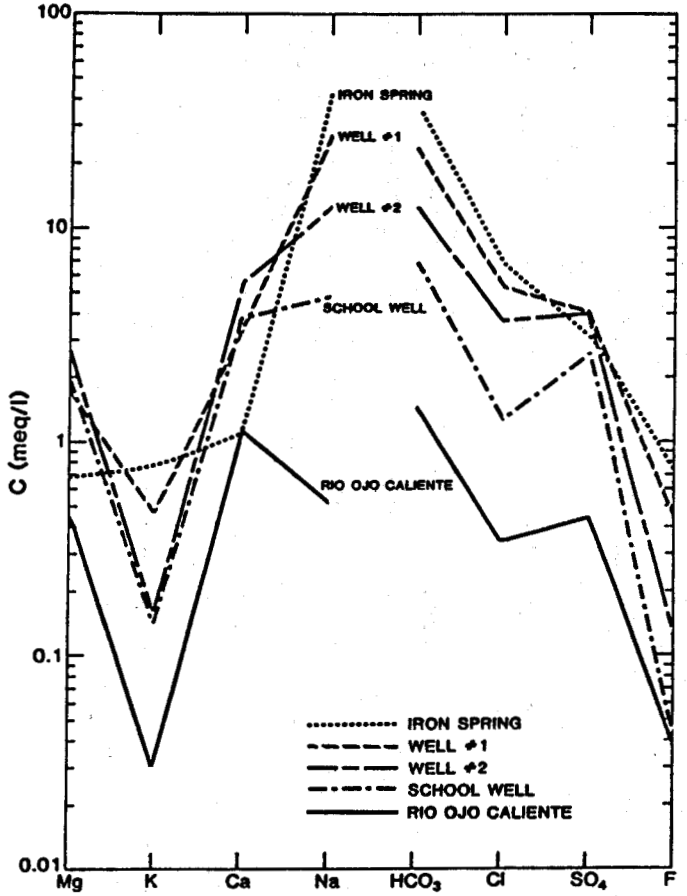

Fig. 5(b).
Ionic composition diagram of the different types of water at Ojo Caliente Resort. Iron spring is representative for the kind of thermal water tapped by the four other warm springs and the Hot well. Wells #1 and #2 show different stages of mixing between ascending thermal water and the shallow aquifer. The latter is supposed to be similar to the School well, whereas the Rio Ojo Caliente is probably typical for the most dilute water percolating into the ground.

4.3.2. Trace Elements. Many trace elements have been analyzed for this study, but because of the fact that all these waters are relatively dilute (TDS = 200 to 3700 mg/ℓ), most of the trace element concentrations are at or below the detection limits of the analytical methods. Traces like Ag, Cd, Co, Cr, Cu, Mo, Ni, NO_3, Pb, and PO_4 are below the detection limit, usually ranging from 0.001 to 0.05 mg/ℓ, for the majority of the samples. Others such as Al, NH_4, and Zn reach and go beyond the detection limit. Finally, Ba, Fe, and Mn have concentrations that are quantitative, whereas the previously mentioned trace elements should be considered as qualitative or semi-quantitative.

Looking at average concentrations, some traces seem to be anomalously high in specific types of water. For example, Ba reaches 0.17 to 0.19 mg/ℓ in wells #1 and #2, representing a mixture between thermal and cold ground water, and surprisingly Ba content is lower in both end-members. Exactly the same phenomenon is repeated for Mn with concentrations of 0.25 and 0.54 mg/ℓ respectively for wells #1 and #2. It is possible that the mixture of the two types of waters has peculiar physico-chemical characteristics, favorable to dissolution of more Ba and Mn minerals. Well #3 has an enormous amount of Fe (35 mg/ℓ), probably explained by the stagnant condition of the water in the casing. Some other water samples have unusually high trace element concentrations, compared to the average values: Mo = 0.09 mg/ℓ at Lowry spring (OC-12), Ni = 0.80 mg/ℓ for Hot well (bottom sample), and Zn = 0.44 mg/ℓ for Statue spring. The rather high contents of Li, B, and F in Ojo Caliente thermal water could come from dissolution of pegmatite minerals in the metarhyolite. Abundant tourmaline, fluorite, and topaz were noted in thin sections of pegmatite and wall rocks in a mine just 1 km north of the warm springs.

4.4 Isotopic Parameters

Oxygen-18 and deuterium data were collected at four different periods from 1974 to 1982 while samples for tritium were taken only in 1982 (Table VI).

4.4.1. Stable Isotopes: Oxygen-18 and Deuterium. Most of oxygen-18 and deuterium values are slightly off the Craig meteoric water line (Fig. 6; Craig 1961). The heaviest isotope values are displayed around the meteoric water

TABLE VI

ISOTOPIC COMPOSITION OF THE WATERS FROM OJO CALIENTE AREA[a]

Name	No.	Date	$\delta^{18}O(°/_{oo})$[b]	$\delta^{2}H(°/_{oo})$[b]	$^{3}H(TU)$
Rio Ojo Caliente	OC-19	4/82	-14.45	-108.5	79±9
Shipap spring	OC-9	7/80	-13.65	-100.3	-
Lower Owl springs	OC-8	7/80	-13.55	-99.8	-
La Cueva spring	OC-7	7/80	-13.70	-98.7	-
Lowry spring	OC-23	4/82	-13.75	-98.9	1.6±0.5
Salt Lick spring	-	7/76	-13.90	-107.1	-
Tap water	OC-6	7/80	-13.60	-102.1	-
Well #1	OC-20	4/82	-13.95	-101.4	18±2
Lithia spring	OC-2	12/79	-14.30	-106.4	-
Iron spring	OC-1	12/79	-14.45	-106.7	-
Sodium Sulfate spring	OC-3	12/79	-14.40	-106.9	-
Iron spring	-	12/74	-14.56	-107.4	-
Sodium Sulfate spring	OC-16	4/82	-	-	1.9±0.6
Arsenic spring	OC-14	4/82	-14.10	-105.7	2.1±0.8
Hot well	OC-4	12/79	-13.65	-102.9	-
Arsenic spring	-	12/74	-14.60	-108.2	-
Hot well	OC-25	6/82	-14.15	-106.2	0.6±0.5
Hot well	OC-18	4/82	-13.10	-101.7	4.3±0.8

[a] The sample arrangement is the same for Tables I and III to VII and is explained in Table III, note a.

[b] Precision of the stable isotopes: $\delta^{18}O = \pm 0.15°/_{oo}$; $\delta^{2}H = \pm 0.5°/_{oo}$.

line and are represented by the springs of La Madera group. The lightest values are those of the Rio Ojo Caliente and the warm springs of the resort.

4.4.1.1. Modifications of the Oxygen-18/Deuterium Relation. Between the warm springs at Ojo Caliente and the wells one can observe a trend with an increasing enrichment in oxygen-18. This shift could be explained theoretically by three different hypotheses: (1) evaporation, (2) mixing patterns between light isotope cold meteoric water and oxygen-18 enriched hot water by a water-rock interaction, (3) connate water.

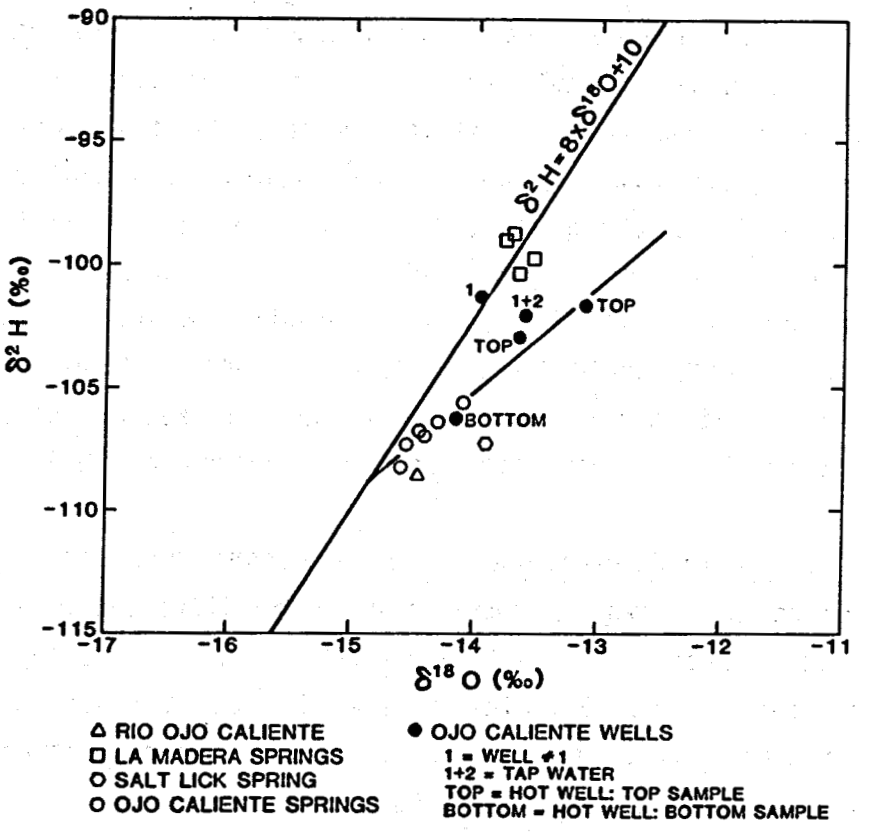

Fig. 6.
Oxygen-18 and deuterium of the waters from Ojo Caliente-La Madera area. Most of the samples are located relatively close to the meteoric water line, but a trend can be observed between the Ojo Caliente warm springs and the Hot well samples taken at the top of the water column. Because of nonflowing conditions and contact with the atmosphere, this trend is presumed to reflect evaporation.

Looking at the type of samples which are most shifted off the meteoric water line, evaporation and therefore a modification of the relation between ^{18}O and ^{2}H seem to be a reasonable explanation (Fontes, in Fritz and Fontes 1980). As a matter of fact, evaporation is very likely to occur in the Hot well, which is not tightly closed at the wellhead. The first two samples (OC-4 and OC-18) were collected at the top of the water column, less than one meter below ground level. The temperature of 54°C and the free contact of stagnant water with the atmosphere naturally leads to evaporation. The last Hot well sample was collected with a well sampler, at the bottom of the hole. The stable isotope values are the same as those of the springs, closer to the

meteoric water line. The sample called tap water (OC-6), which is a mixture of thermal water with shallow local ground water, was collected during the summer in a tank used for potable water supply. Although this mixture is about 30% less mineralized than the thermal water, the same type of isotopic shift can be seen, giving more weight to the evaporation hypothesis. On the other hand, the well #1 alone (OC-20), with same mineralization as OC-6, sampled at the wellhead during pumping shows absolutely no shift.

North of La Madera, Salt Lick spring isotopic composition, shifted from the meteoric water line, could be caused by mixing of dilute local ground water and a mineralized connate water, of which the isotopic composition was modifed either before its percolation into the ground or within the porous medium.

4.4.1.2. Recharge Elevations. Correlations between isotopic and chemical parameters are shown in order to decipher different water components mixing in various degrees. The most conservative ion and isotope, namely Cl and ^{2}H, are related in Fig. 7. The same mixing pattern already known with physical and chemical parameters can be observed here between the warm springs, the bottom-hole sample of the Hot well and the well #1 and the tap water. The two top Hot well samples, which went under evaporation, and the

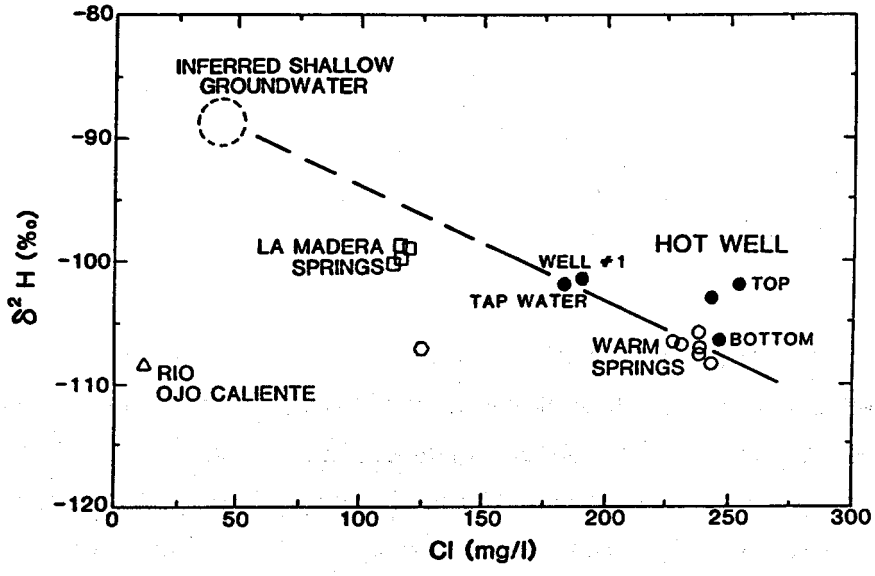

Fig. 7.
Deuterium and chloride correlation. Extrapolation of the trend between the warm springs and the mixed water of the shallow wells at the resort toward the low chloride content do not show a deuterium value similar to that analyzed for the river. This discrepancy might be caused by changes in the water isotopic composition during the hydrologic cycle due to high- or low-elevation origin within the drainage basin (summer rainfall or snowmelt).

group of La Madera springs, which are not thought to be related with the Ojo Caliente thermal water system, are not taken into consideration. Extension of the mixing line towards more dilute water, supposedly the uncontaminated shallow ground water such as the School well (Cl = 45.5 mg/ℓ), shows a strong deuterium increase (δ^2H = -88°/₀₀). Furthermore, this value is very different from the Rio Ojo Caliente (-108°/₀₀), whose water is likely to feed the valley alluvium aquifer.

At the time of the sampling in the creek, the waters were high due to snowmelt in the upper part of the basin (about 2700-3300 m), and consequently show a low deuterium value. On the other hand, the water in the alluvium mixing with deep thermal water probably is buffered and shows weak seasonal changes. Alternatively it may have contained the water infiltrated the previous summer or fall. This means a much lower apparent recharge basin for the shallow ground water, and that would markedly raise the deuterium content. However, more isotopic analyses of the shallow aquifer, mixed as well as uncontaminated samples, are needed to confirm this hypothesis.

Finally, the recharge zone of the warm springs should be at high elevation, probably around 3000 m compared with the snowmelt value for the Rio Ojo Caliente. Sampling of the warm springs at different periods of the hydrologic cycle and for different years reveals only slight differences, facts which indicate a well-buffered system.

4.4.2. Radioactive Isotope: Tritium.

4.4.2.1. Tritium in Surface Water. Before the first atmospheric nuclear tests (1953), the natural production of tritium measurable in surface water reached 5-10 TU. In 1963, artificial tritium concentrations peaked to about 1000 TU in surface waters and several thousand TU in precipitation. Since the moratorium on atmospheric tests, tritium content has been decreasing. Six stations for precipitation (Utah, Colorado, Arizona, and New Mexico) and two stations on the Colorado River (Utah and Arizona-California border) are averaged and plotted on a histogram showing the evolution of tritium content in the surface waters of the southwestern United States as a function of time (Fig. 8). During the last five years (1978-1982), tritium content in precipitation has fallen from 75 to 40 TU and in river water from 110 to 60 TU (WATSTORE 1983).

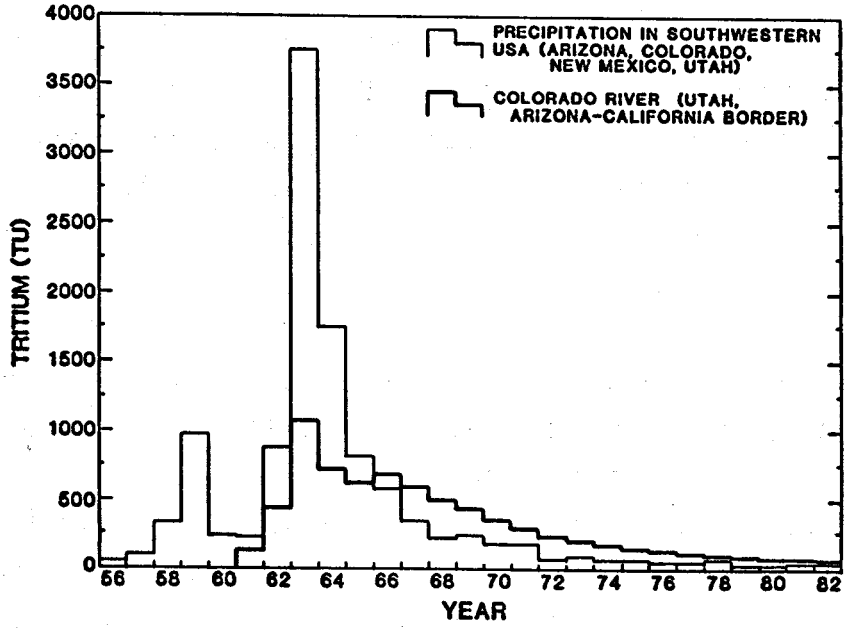

Fig. 8.
Tritium-time variations in southwestern U.S., using data from regional precipitations and the Colorado River. The thin line represents the yearly average tritium concentration for one to six precipitation stations according to the available data (Salt Lake City, Utah; Denver, Colorado; Flagstaff, Arizona; Albuquerque, New Mexico; Socorro, New Mexico; Mt. Withington, New Mexico). The thick line represents the yearly average tritium concentration for one to two stations on the Colorado River (Cisco, Utah; above Imperial Dam, Arizona-California border). All values are from a data bank of the U.S. Geol. Survey (WATSTORE 1983).

Using the 12.3 yr half-life period of tritium and the records of tritium content in surface waters from previous years, it is possible to date or at least to give an order of magnitude of the age of ground waters. For this study, one surface water, namely the Rio Ojo Caliente, has been analyzed for tritium. In early April 1982, its concentration reached 79±9 TU. This value is higher than the average 71±3 TU calculated from the two stations on the Colorado River, covering the six previous months from October 1981 to March 1982 (WATSTORE 1983), but this 10% difference is probably due to regional climatic and topographic effects (Fontes, in Fritz and Fontes 1980).

4.4.2.2. Tritium in Ground Water. Except for well #1, a mixture of deep thermal and shallow cold ground waters, which has a tritium content of 18±2 TU, the warm springs and the Hot well have a very low tritium concentration ranging from 0.6 to 4.3 TU (Table VI). The latter value comes from the top sample of the Hot well and indicates atmospheric contamination. A small

amount of rain or snow could infiltrate through the wellhead, which is closed by a board and a stone. In contrast, the bottom-hole sample of the Hot well contains almost no tritium (0.6±0.5 TU), indicating the presence of water primarily infiltrated before the first atmospheric nuclear test (Table VI). Assuming a pre-bomb tritium content of 5 to 10 TU in precipitation, 40 to 50 years without any atmospheric contact are necessary for tritium decay to reach 0.6 TU. This means that the thermal water emerging at Ojo Caliente Resort may have infiltrated into the ground during the 1930's or the 1940's. However, thermal water may be totally tritium free, having been in the ground for 70 to 80 years or more and being slightly contaminated by recent ground water.

A mixing trend between old mineralized and young dilute ground water has been established with the bottom-hole Hot well, the two warm springs, and well #1 (Fig. 9). Extension of this trend towards greater dilution reaches the tritium and Cl contents of surface water and therefore indicates (1) the Rio Ojo Caliente type of water might feed the shallow local ground water, and (2) the warm springs flowing naturally at the surface are actually pre-bomb water, slightly contaminated by tritiated water in the emergence zone.

One sample from the La Madera group of lukewarm waters, Lowry spring, also reveals a very low tritium concentration of 1.6 TU. Unless other samples

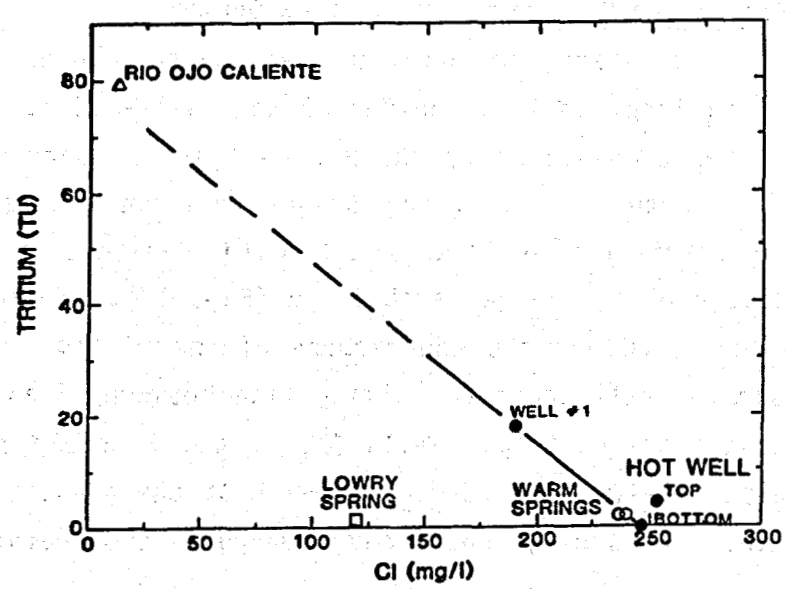

Fig. 9.
Tritium and chloride correlation. Extrapolation of the trend between the undiluted thermal water and the mixed shallow aquifer approaches the high tritium content of the surface water, which is likely to feed the alluvium aquifer.

will be analyzed in the same area, two explanations are possible: either Lowry spring was originally tritium free and then slightly contaminated during water ascent by shallow recent ground water, or its water percolated into the ground 30 years ago, just before the first nuclear tests.

5. RESERVOIR TEMPERATURE

Naturally it is of high interest in a study on geothermal potential to estimate deep temperature of the fluids, which can be tapped at depth by drill holes. In most cases, during thermal water ascent from a nonboiling reservoir toward surface, temperature losses occur by conductivity and/or by mixing. Temperature differences between the reservoir at depth and the emergence at surface or in a shallow aquifer essentially depends on the types of channels and openings used as flow paths by the ascending waters. A small temperature drop will be observed from a large flow rate (>100 ℓ/min) emerging from a single fracture. On the other hand, small discharges or geologic and tectonic structures leading to small springs or seeps widespread over a large area can almost suppress its thermal characteristics. Finally, mixing with shallow cold ground waters is frequently encountered in various geologic environments (Vuataz 1982; Vuataz et al. 1983).

5.1 Cooling by Mixing and Conduction at Shallow Depth

In the previous chapters, mixing has been shown between the ascending thermal water and the local shallow aquifer of the valley fill. Assuming that the 55°C thermal water encountered by the Hot well is the highest temperature possible at shallow depth, and that the School well represents the physical and chemical characteristics of the local cold aquifer, a mixing model including conductive cooling can be established (Fig. 10). These two types of ground water are considered as the end-members of the mixing. All the other well and spring samples fall under the mixing line between Cl and temperature, which indicates conductive cooling. Wells #2, 1, and 3 should reach a mixing temperature of respectively 31, 43, and 57°C without the additional conductive cooling, whereas the warm springs could have emergence temperatures between 51 and 55°C.

Starting from the Hot well and going northeast (upstream on the Rio Ojo Caliente and also upgradient in the shallow aquifer; Figs. 1 and 3), an increasing differential cooling is observed. Emergence temperatures of 34,

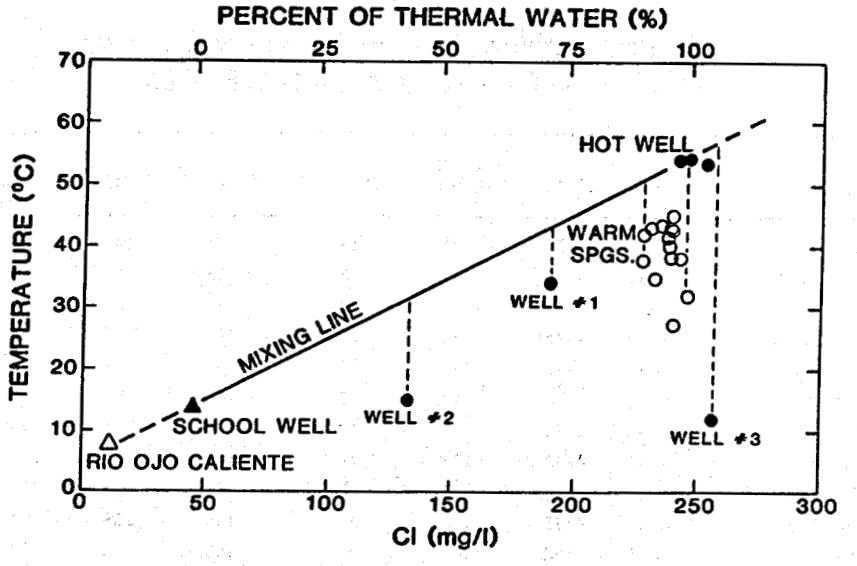

Fig. 10.
Emergence temperature versus chloride and estimation of mixing percentage. A mixing line links the two inferred end-members, allowing determination of the percentage of thermal water according to the chloride concentration. All the water samples undergo strong conductive cooling, even the less diluted ones.

15, and 12°C were measured for wells #1, 2, and 3. Indeed, they are conductively cooled by 9, 16, and 45°C, respectively, according to the mixing model. This may be because of both decreasing influence of the thermal water plume zone and the pressure of the flowing cold aquifer.

5.2 Chemical Geothermometry

Using the concentration and the ratios of temperature-dependent chemical species, deep reservoir temperatures can be evaluated. Experimental studies have been done on SiO_2, and empirical relationships have been established for the elements Li, Na, K, Ca, Mg, and their ratios. The so-called geothermometers are now widely used in water geochemistry for geothermal exploration (see complete references in Table VII).

Before using these geothermometers to calculate any deep temperatures, their limits of application must be known, as well as certain basic assumptions on the hydrologic system. Fournier (1977) summarized these assumptions: (1) Temperature-dependent water-rock interactions fix the content of the dissolved indicator in the water. (2) Supply of the reactants is not limited. (3) Specific indicator reactions are at equilibrium in the

TABLE VII

CHEMICAL GEOTHERMOMETRY (°C) OF SELECTED SAMPLES FOR THE WATERS OF OJO CALIENTE AREA[a]

Name	No.	Date	Quartz[b] conduc.	Chalced.[c]	T Na/Li[d]	T Na/K[e]	T NaKCa[f]	T NaKCa[g] (Mg)
School well	OC-27	6/82	87	56	118	163	53	-
Statue spring	OC-26	6/82	69	37	135	212	77	37
Shipap spring	OC-9	7/80	65	33	-	206	75	52
Lower Owl spring	OC-11	11/81	65	33	141	197	73	54
La Cueva spring	OC-7	7/80	85	54	-	194	70	60
Lowry spring	OC-23	4/82	57	25	144	196	72	54
Salt Lick spring	OC-10	11/81	81	49	176	97	81	81
Lithia spring	OC-13	4/82	108	79	164	135	149	60
Sodium Sulfate spring	OC-16	4/82	111	82	166	131	148	66
Arsenic spring	OC-14	4/82	110	80	165	135	150	64
Iron spring	OC-15	4/82	111	82	160	135	150	64
Soda spring	-	1891-93	111	81	157	135	151	57
Soda spring	-	10/49	115	86	-	130	146	61
Soda spring	OC-17	4/82	112	83	163	131	148	67
Hot well	OC-25	6/82	114	86	156	135	153	79

[a] The sample arrangement is the same as for Tables I and III to VII and is explained in Table III, note a.

[b] Quartz geothermometer with conductive cooling (Fournier and Rowe 1966; Fournier in Rybach and Muffler 1981)

[c] Chalcedony geothermometer (Fournier 1973; Arnórsson 1975)

[d] T Na/Li geothermometer (Fouillac and Michard 1981)

[e] T Na/K geothermometer (Fournier 1979; White 1970)

[f] T NaKCa geothermometer (Fournier and Truesdell 1973). The temperatures below 100°C were calculated with $\beta = 4/3$, whereas $\beta = 1/3$ was used to obtain the temperatures above 100°C.

[g] T NaKCa Mg-corrected geothermometer (Fournier and Potter 1979)

reservoir. (4) No reequilibration takes place during water ascent. (5) No mixing occurs or if that happens, its result can be quantitatively evaluated.

The main geothermometers have been calculated for each type of water at Ojo Caliente (Table VII). Among the SiO_2 geothermometers, the authors agree that above 100°C, quartz controls aqueous SiO_2 solubility (Fournier, in Rybach and Muffler 1981), whereas chalcedony is more likely to be encountered for waters under 100°C (Arnórsson 1975; Michard and Fouillac, in Tardy 1980). Temperatures calculated with Na/Li and Na/K geothermometers are listed here only for comparative information because they do not give reasonable results for nonboiling reservoirs. The Na-K-Ca geothermometer has been established for calcium-rich waters in regards to Na and K, and works for a wide range of reservoir temperatures. In case Mg is relatively important in comparison to K and Ca, a specific correction factor should be applied.

None of the thermal waters studied at Ojo Caliente and surroundings are believed to reach a reservoir temperature above 100°C at present times, because no indicator of high temperatures is present, namely intense hydrothermal alteration of rocks, sinter deposits, high gas content in water, and high B and NH_4 concentration. The bottom-hole sample of the Hot well (OC-25) has been considered as the unmixed end-member for its physical, chemical, and isotopic characteristics. Therefore, the temperature of 86°C computed with the chalcedony geothermometer is thought to be the maximum subsurface reservoir temperature.

A slightly lower temperature of 79°C is given by the Na-K-Ca Mg-corrected geothermometer. This difference of 7°C is within the error of the geothermometers. The solubility of magnesium minerals is very temperature dependent (Garrels and Dreyer 1952), a fact which is confirmed by the analyses of Ojo Caliente thermal water. In the five warm springs, Mg content averages around 8.1 mg/ℓ for a mean temperature of 39°C, whereas the bottom-hole sample of the Hot well reaches only 5.4 mg/ℓ at 55°C. One can assume that during thermal water ascent, Mg minerals are dissolved proportionally to the cooling of the water, and consequently, Mg concentration may change rapidly due to emergence conditions. Therefore, a 7°C difference is probably not significant between the chalcedony and Na-K-Ca Mg-corrected geothermometers. In conclusion, the maximum reservoir temperature of the Ojo Caliente thermal water is thought to reach about 85±5°C, 30°C above the recorded temperature.

Considering now the lukewarm and dilute waters of the La Madera springs group, it is necessary to compare their SiO_2 concentration with that of the cold waters (Rio Ojo Caliente, School well, and Salt Lick spring). The five lukewarm springs have a SiO_2 content ranging from 17 to 34 mg/ℓ, whereas the three cold waters have higher SiO_2 values from 22 to 36 mg/ℓ. This comparison does not allow use of the chalcedony geothermometer on these dilute waters, which probably derive from these already silica-rich surface or shallow waters. The other geothermometers are unlikely to be significant for this relatively cold system. If any of the La Madera springs is warmer at depth, it is unlikely that the reservoir temperature would reach more than 30-40°C.

6. CHEMICAL EQUILIBRIA

Chemical compositions of ground waters depend on their interactions with reservoir rocks such as granite, sandstone, limestone, etc. and on parameters such as temperature and pressure, time available for chemical reactions, rate of fluid flow, and water-rock ratio. The original composition of a thermal water ascending from its deep reservoir toward surface may be modified by precipitation or dissolution of minerals, because of changes in the above mentioned parameters. The reaction states of the fluid, namely undersaturated, saturated, or oversaturated with respect to a solid mineral phase, can be calculated from a chemical equilibrium model. Kharaka and Barnes (1973) established a computer program, SOLMNEQ, which calculates states of reaction of numerous mineral aqueous species generally present in natural waters over the temperature range of 0 to 350°C, with respect to 158 solid mineral phases for which thermodynamic data are available. The input consists of the chemical analysis as well as the fluid temperature, the pH, and the Eh. The output indicates, among other computed parameters, the change in the Gibbs free energy (ΔG, kcal/mol) (Barnes and Clarke 1969). Positive values of ΔG computed by the program indicate that the fluid is oversaturated with respect to the mineral and that this mineral may precipitate, whereas negative ΔG values indicate that the water is undersaturated with respect to that phase, which could dissolve in solution. Equilibrium between a mineral and water is theoretically attained if the Gibbs free energy equals zero (±2 kcal/mol for this discussion). However, this cannot be taken as an absolute indication that a particular mineral is dissolving or precipitating. A favorable kinetic rate might allow the precipitation of a thermodynamically less stable phase, at the expense of a thermodynamically stable phase that has an unfavorable kinetic rate (Grigsby et al. 1983).

6.1. Water-rock Interaction

Chemical analyses of two springs of the La Madera group, three springs and two wells from Ojo Caliente were processed through the computer program SOLMNEQ to calculate the Gibbs free energy changes. The reaction states for 25 selected minerals, which might be expected to participate in water-rock interactions, are reported in Table VIII.

The two springs selected from the La Madera group appear to be saturated ($-2 \leq \Delta G \geq +2$ kcal/mol) with respect to many minerals, all the forms of SiO_2,

TABLE VIII

REACTION STATES OF DISSOLVED MINERALS FOR SELECTED WATERS OF OJO CALIENTE AREA. VALUES LISTED ARE GIBBS FREE ENERGY DIFFERENCE AT EMERGENCE TEMPERATURE (kcal/mol).

	Mineral phases	Shipap spring OC-9	Lower Owl springs OC-8	Lithia spring OC-2	Iron spring OC-1	Arsenic spring OC-5	Hot well OC-25	Well #3 OC-28
Primary silicates	Albite High	-7.4	-2.1	-3.0	-3.6	-0.84	-0.18	-2.1
	Anorthite	-14	-3.6	-9.0	-9.8	-4.1	-2.3	-9.2
	Microcline	-4.2	1.2	-0.58	-1.3	1.5	1.9	0.66
	Quartz	0.67	0.75	1.1	1.0	1.1	1.8	1.4
	Biotite Fe	-18	-8.0	-7.3	-2.9	-2.2	7.3	6.7
	Muscovite	1.2	16	7.1	5.7	13	14	8.4
Secondary silicates	Albite Low	-6.0	-0.66	-1.7	-2.3	0.52	1.1	-0.61
	Chalcedony	0.09	0.16	0.57	0.51	0.52	0.42	0.80
	Cristobalite α	-0.17	-0.10	0.30	0.24	0.25	0.14	0.54
	Illite	-6.2	5.1	-1.2	-2.4	3.7	4.2	-0.07
	Kaolinite	-3.1	6.1	-0.03	-0.87	4.1	3.8	0.73
	Montmorillonite Na	-4.5	6.6	0.42	-0.64	5.3	5.1	1.5
	Laumontite	-5.7	4.7	-0.89	-2.2	3.5	4.8	0.66
	Phillipsite	7.9	13	12	11	14	14	13
	Marialite	-11	5.4	3.4	1.5	9.8	12	7.3
Sulfates, carbonates, fluoride	Fluorite	-0.64	-0.75	0.58	0.49	0.68	0.43	1.2
	Calcite	-1.0	-0.60	-0.70	-0.92	-0.67	0.17	-0.11
	Aragonite	-1.1	-0.66	-0.76	-0.99	-0.74	0.09	-0.15
	Dolomite	-1.9	-0.97	-1.1	-1.7	-1.1	0.53	-0.93
	Witherite	-0.27	0.33	1.6	1.4	1.8	2.5	2.8
	Siderite	-3.8	-2.7	-1.7	0.11	-1.0	1.1	2.7
	Strontianite	-0.89	-0.37	1.0	1.1	1.4	2.7	1.6
	Gypsum	-1.2	-1.2	-2.9	-3.1	-3.1	-3.6	-2.8
	Barite	-0.53	-0.40	-0.52	-0.66	-0.45	-0.85	-0.07
	Celestite	-2.7	-2.5	-3.0	-3.1	-3.1	-3.3	-2.9

the Ca-, Mg-, Ba- and Sr-carbonates, the Ca- and Ba-sulfates, as well as fluorite. This may show the deep water reaches the surface without mixing with dilute shallow water, as already confirmed by the very low tritium content of Lowry spring. Aluminosilicates like K-feldspars, clays, zeolites, and scapolites are either under- or oversaturated, strongly dependent on the ionized Al^{+3} content analyzed in the water. Not enough Al^{+3} data are available to use an average value. Phillipsite, a Ca-zeolite, is the only common oversaturated mineral, but it is unlikely to precipitate at such low emergence or even reservoir temperatures (25-35°C). Plagioclase, biotite-Fe, siderite, and celestite are observed to be undersaturated. The latter mineral is very soluble, therefore, Sr and SO_4 concentrations should reach 10-15 mg/ℓ

and 2000-4000 mg/ℓ, respectively, in a strongly mineralized water to be saturated (Goff et al. 1983). Lower Owl springs water is oversaturated with respect to muscovite, some clays, and zeolites. In short, the La Madera waters will merely dissolve most primary silicates and could only possibly participate in low-temperature diagenetic reactions.

The five waters selected for Ojo Caliente display similar results, although their emergence temperature ranges between 12 and 54°C (Table VIII). Again, numerous mineral phases appear to be in the saturation range, arbitrarily fixed from -2 to +2 kcal/mol. These are mainly the silica minerals, clays, carbonates, fluorite, and sulfates, except gypsum and celestite. The primary minerals of a metarhyolite being quartz, K-feldspars, muscovite, and a small quantity of Na-plagioclase, it appears that the thermal water is either saturated or oversaturated with respect to these minerals. This may confirm the absence of dilution of the thermal water. Among the saturated to oversaturated minerals, zeolites and clays are observed; but they strongly depend on their Al^{+3} content. Again, the Al^{+3} data are scarce and further studies would be needed to ascertain the equilibrium states for aluminosilicates, but indications are that the Ojo Caliente fluids are not participating in any significant reactions with reservoir rocks except low-temperature reactions.

6.2 Variation of Equilibria with Temperature

In case of future drilling in the thermal water reservoir at Ojo Caliente for space heating, it is of prime interest to know if any mineral will precipitate in the heat exchangers, pipes, and other surface equipment. A new drill hole is likely to tap warmer water at a temperature somewhere between emergence temperature (55°C) and inferred reservoir temperature (85°C). Therefore, the reaction states of the thermal water (Hot well, bottom-hole sample, OC-25) were computed for temperatures of 55, 65, 75, 85, and 95°C, in order to evaluate the effect of temperature on mineral solubilities. The Gibbs free energy changes are then plotted against temperature for a selection of mineral phases which are close to the saturation state (Fig. 11). All minerals but calcite display a decreasing ΔG with increasing temperature. Silicates become more soluble at a faster rate than silica, fluorite, and sulfates. Calcite, as well as other carbonates like aragonite, dolomite and siderite become slightly less soluble while temperature increases. On the other hand, the Ba-carbonate (witherite) and the Sr-carbonate (strontianite)

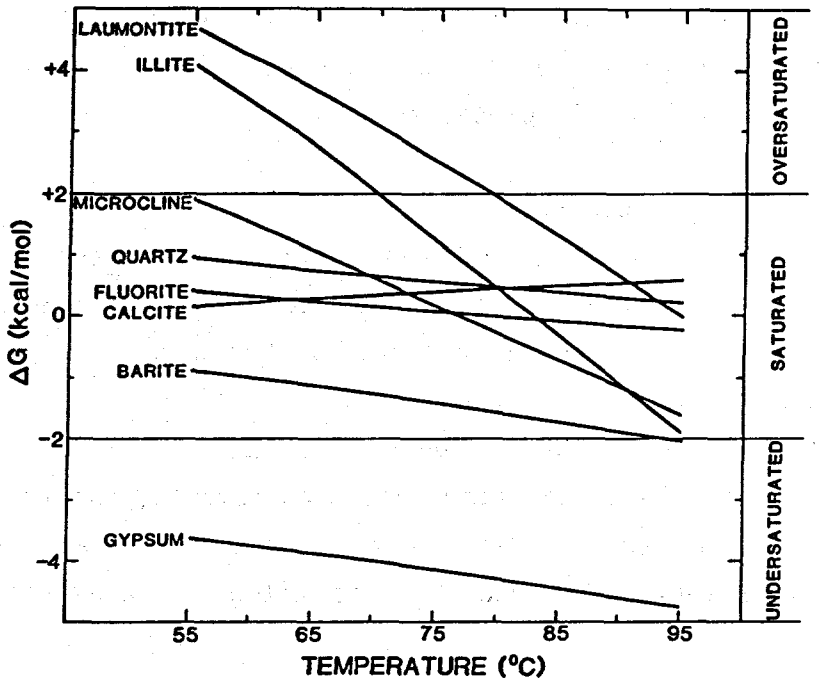

Fig. 11.
Variation of Gibbs free energy changes with temperature. The reaction states are plotted for eight mineral phases from the Hot well (OC-25) fluid chemistry. The range of saturation limits has been set arbitrarily at 0±2 kcal/mol, because other factors than thermodynamics affect precipitation or dissolution. Each line is drawn with five values calculated for 55, 65, 75, 85, and 95°C.

behave differently: the first one is observed to increase its solubility with temperature, whereas the second one is stable.

None of the ground waters studied here seem to have built the Quaternary travertine deposits observed in the Ojo Caliente-La Madera region. No active concretion was encountered by the emergence zone; only a red stain is observed around the warm springs at the Resort, due to iron precipitation. All the waters are Na-HCO_3 and not Ca-HCO_3 type, and they do not display high positive values of ΔG for calcite state of reaction. It is most likely that the waters responsible for the travertine deposits were flowing during a period of higher hydrothermal activity and have run dry since then. However, it might be possible that the low discharge springs around La Madera could slowly build travertine terraces by evaporation.

In conclusion, the thermomineral water that may be tapped at higher temperatures by a deeper well around Ojo Caliente to be used for space heating will not cause much trouble in the wells or in the surface equipment. Indeed,

this water is neither particularly aggressive nor incrustant. It appears to be incapable to dissolve or deposit an important amount of mineral phases, especially if the plumbing is a closed system.

7. PUMPING TEST IN THE HOT WELL

In October 1981, a pumping test was carried out in the Hot well by Rio Grande Well Supply Company of Santa Fe, New Mexico. It was not part of this study program and the following interpretation has been made possible through the data released by the Ojo Caliente Resort.

This pumping test lasted only about six hours. Nothing is known about the precision of the water level and flow rate measurements, the recovery of water level was not observed, and no water samples were collected. Moreover, the pumping steps were very short and did not allow a steady-state flow to be reached.

7.1 Well Characteristics

Very little can be interpreted from this pumping test, due to the lack of basic data, but also because this well was supposedly not drilled for the purpose of tapping hot water but for potable water supply. According to the driller's log (Summers 1976), when the hot water was struck at 26.5-m depth, the drilling was stopped. At 15 m the water was said to be cold, tapping the valley alluvium aquifer such as wells #1 and #2.

The Hot well is 26.5 m deep, the casing is a 17.8-cm (7-in.) i.d. steel pipe inserted inside a 22.9-cm (9-in.) i.d. steel pipe. Nothing is known about packers, screens, or slotted liners. A submersible pump was set at 12.6-m depth only, because of a blockage encountered at 13.5 m below surface. The initial water level in the well before any pumping was 1 m below ground level. During the entire pumping cycle, the water temperature remained constant at 53.3°C; but the precision of this value is unknown. Six different short pumping tests were carried out with pumping times of 5 to 115 minutes and discharges between 23 to 83 ℓ/min. At the highest discharge of 83 ℓ/min, the drawdown reached the pump level in 10 minutes. Then the pump was shut down for only 20 minutes to allow the well to recover before continuing with the pumping test.

The specific capacity of the well, which is the flow rate (ℓ/min) obtained by unit of drawdown (m) (Freeze and Cherry 1979), varied during the

pumping from 7 to 18 ℓ/min•m according to the various flow rates. At the end of the three longest steps, the specific capacity was each time more or less stabilized at 11 ℓ/min•m. This means a 10-m drawdown for about 100 ℓ/min, which is a major drawdown for a very small discharge.

The critical yield for a given well is the maximum production pumping rate and can be defined graphically by the relation between flow rate and stabilized drawdown (Fig. 12). The critical yield is fixed at the inflection point of the curve when the relation becomes nonlinear. For the Hot well, the critical yield is estimated to be 65±5 ℓ/min, a very small value for a 26-m-deep well with a 17.8-cm i.d. casing.

7.2 Aquifer Characteristics

By means of the data obtained during the longest step at the same rate (115 minutes at 57 ℓ/min), one can calculate the transmissivity of the aquifer, using the Jacob's method for unsteady-state flow in confined aquifers (Kruseman and De Ridder 1979). The transmissivity is the product of the average permeability (or hydraulic conductivity) and the thickness of the aquifer. Therefore, transmissivity is the rate of flow under a hydraulic gradient equal to unity through a cross section of unit width over the whole thickness of the aquifer. It is designated by the symbol T and expressed in m^2/day. The drawdown is plotted against the pumping time on logarithmic scale; and the slope, namely the drawdown difference per log cycle of time, is entered in the Jacob's formula with flow rate (Fig. 13). This is an approximation of the method, because the drawdown was measured in the pumped well itself, instead of an observation well located in the influence area of the pumping. The transmissivity value of 15 m^2/day found for this pumping test is at least 10 times smaller than average

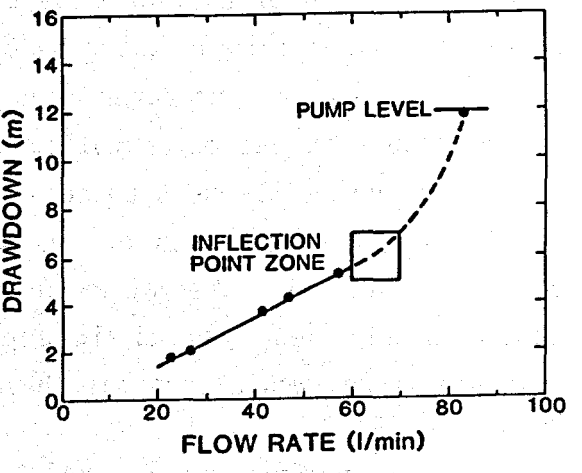

Fig. 12.
Determination of the critical yield of the Hot well. A pumping test at various flow rates allows location of the inflection point on the curve obtained by the relation between stabilized drawdown and pumped flow rate data. A few values are missing between 57 and 83 ℓ/min but it is evident that the critical yield would not exceed 65±5 ℓ/min.

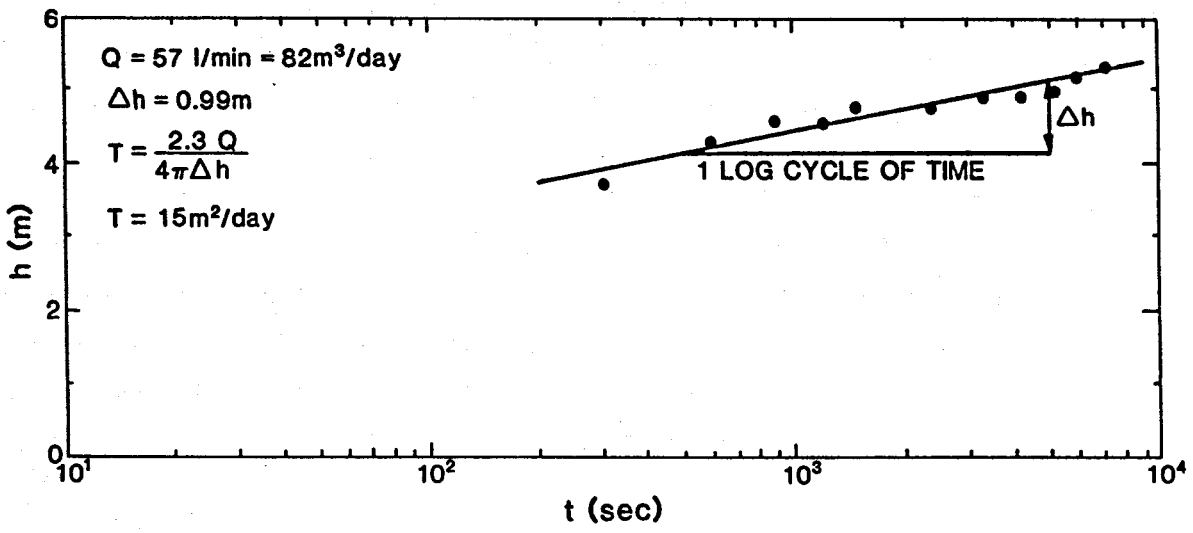

Fig. 13.
Determination of the transmissivity. Using the longest pumping step, the drawdown values (h) are plotted against the pumping time (t) on a logarithmic scale. The drawdown difference (Δh) for one logarithmic scale of time is entered in Jacob's formula with the flow rate (Q) to calculate the transmissivity (T).

transmissivity for this size of well. Because no data are available on the thickness of the production zone struck by the Hot well, the permeability (or hydraulic conductivity) cannot be calculated.

It has to be remembered that the production zone is not a porous medium but a fissure in the metarhyolite or a series of small joints, and the drilling of the Hot well was stopped when it hit the warm water. This explains the very poor characteristics of the well and of the "aquifer" in the immediate vicinity. A deeper thermal water well, which would be located on the basis of geologic and geophysical interpretation and penetrate deeper into the fractured zone, would certainly have much better characteristics and yield.

8. SHALLOW TEMPERATURE SURVEY

In June 1982, a network of 24 shallow holes was drilled with an auger for the purpose of conducting an experiment using a new technique to measure average subsurface temperatures for a long period of time (Faler et al. 1980). These holes have a mean depth of 1.2±0.3 m and are cased with plastic tubing. Other plastic tubes containing vials of temperature-sensitive chemicals were lowered into the casing and left for a period of three months. Another set of samples stayed in the casing for nine months. These samples were analyzed to

evaluate the extent of the kinetic reaction, data which give an indication of the soil temperature around the samples, averaged over the entire time that the samples were left underground. This system is capable of measuring mean temperature difference of about 0.1°C. The interpretation of these measurements are not completed (G. Wiegand and G. Heiken, Idaho State University and Los Alamos National Laboratory, unpublished data, 1983).

During the pull-in and the pull-out of the chemical samples, instant temperatures were measured at the bottom of the holes with temperature probes and digital thermometers. Three series of measurements for three different periods are reported in Table IX, with electrical conductivity values, measured in the holes containing enough water. A map of the isotherms based on the average of the three temperature recordings displays few anomalies numbered I to IV (Fig. 14). At Ojo Caliente Resort itself (I), the temperature at 1.2±0.3 m deep varies between 20 and 25°C, with the maximum in the seepage area, about 150 m northwest of the warm springs. At surface the seep water is relatively cold (~16°C) but contains as much mineralization as the warm springs water. On the west side of the Rio Ojo Caliente, about 1.3 km upstream from the resort (II), another temperature anomaly peaks at 19°C. If this anomaly was caused by differential aquifer temperatures from seasonal changes and river infiltration, the isotherms probably would be parallel to the stream. A smaller anomaly can be observed between the first one and the resort (III) reaching only 16°C, but with the same isotherm shape crossing the river. Finally a temperature increase is seen 600 m downstream from the resort (IV), also on the west bank of the Rio Ojo Caliente. However, contrary to the previous anomalies (II and III), the temperature decreases toward the river.

The few electrical conductivity values available corroborate the temperature anomalies (Table IX). Keeping in mind that the electrical conductivities of the Rio Ojo Caliente and the uncontaminated shallow aquifer upstream of the warm springs are respectively 200 and 1000 µS/cm, one can observe the following conductivity anomalies. (I) Values of 4100 to 4500 µS/cm indicate practically 100% of thermomineral water. Hole #13 with 1900 µS/cm is similar to the nearby well #2 (OC-21). (II and III) Maximum values of 1300 µS/cm correspond to a small percentage of thermomineral water in the aquifer. (IV) Two values of 1900 and 2300 µS/cm probably suggest a downstream plume of thermomineral water in the alluvium aquifer.

TABLE IX

MONITORING OF SHALLOW TEMPERATURE HOLES AT OJO CALIENTE

Holes		June 18, 1982		August 26, 1982		June 23, 1983		Mean temperature (°C)
No.	Depth (m)	T(°C)[a]	water[b]	T(°C)[a]	K(μS/cm)[c]	T(°C)[a]	K(μS/cm)[c]	
1	2.0	11.5	±	17.2	--	12.5	--	13.7
2	1.22	14.7	-	17.6	--	14.2	--	15.5
3	1.22	15.4	-	17.4	--	14.6	--	15.8
4	0.91	15.1	-	18.2	--	15.6	1200	16.3
5	1.52	17.0	-	20.2	--	15.8	2300	17.7
6	1.37	17.3	-	21.3	--	19.4	--	19.3
7	1.07	--	-	18.3	--	15.2	1900	16.8
9	1.37	20.8	-	25.7	4500	21.1	4500	22.5
10	1.37	21.9	-	25.5	4400	22.9	4400	23.4
11	1.52	23.2	+	28.6	4300	24.5	4100	25.4
12	1.22	21.6	-	24.0	--	21.6	--	22.4
13	0.91	22.2	-	25.0	--	23.0	1900	23.4
14	0.91	20.8	-	27.3	--	22.3	--	23.5
15	1.07	20.4	-	22.9	--	20.4	--	21.2
16	0.76	14.0	+	17.1	--	14.8	1100	15.3
17	0.91	15.9	+	19.6	wet	17.3	1300	17.6
18	0.76	18.2	-	20.1	--	17.3	wet	18.5
19	0.99	15.2	-	19.0	--	16.6	--	17.2
20	1.52	15.4	-	17.5	--	15.5	--	16.1
21	1.52	14.7	±	17.8	--	14.8	1300	15.8
22	1.22	13.6	-	16.0	--	13.2	--	14.3
23	1.52	14.8	+	17.3	wet	15.6	1300	15.9
24	1.52	13.9	-	16.7	wet	13.4	1300	14.7
25	0.61	19.7	-	21.7	--	19.8	wet	20.4
$\bar{X}$[d]	1.2	17.3		20.6		17.7		18.5
σ_X[d]	0.3	3.3		3.8		3.6		3.5

[a] The temperature values in the dry holes were measured after waiting 5 minutes for stabilization. In the holes containing water, stabilization occurred much faster.

[b] Presence of water at the bottom of the hole: + = water; ± = damp; - = dry.

[c] Electrical conductivity measured by lowering a probe to the bottom of the hole.

[d] Averages and standard deviations for the depth and the bottom hole temperatures. Although hole #7 has been measured twice, it has not been taken into consideration for the four general averages, to remain consistent.

9. RESISTIVITY SOUNDINGS

To map the hot water underlying the Ojo Caliente area, eight Schlumberger D.C. resistivity soundings were conducted in the Rio Ojo Caliente valley within a few kilometers of the warm springs. The location of the survey points are shown on the geologic map (Fig. 2). When interpreted, these soundings allow inference of the earth's resistivity as a function of depth underneath the survey point. These surveys are effective in locating hot

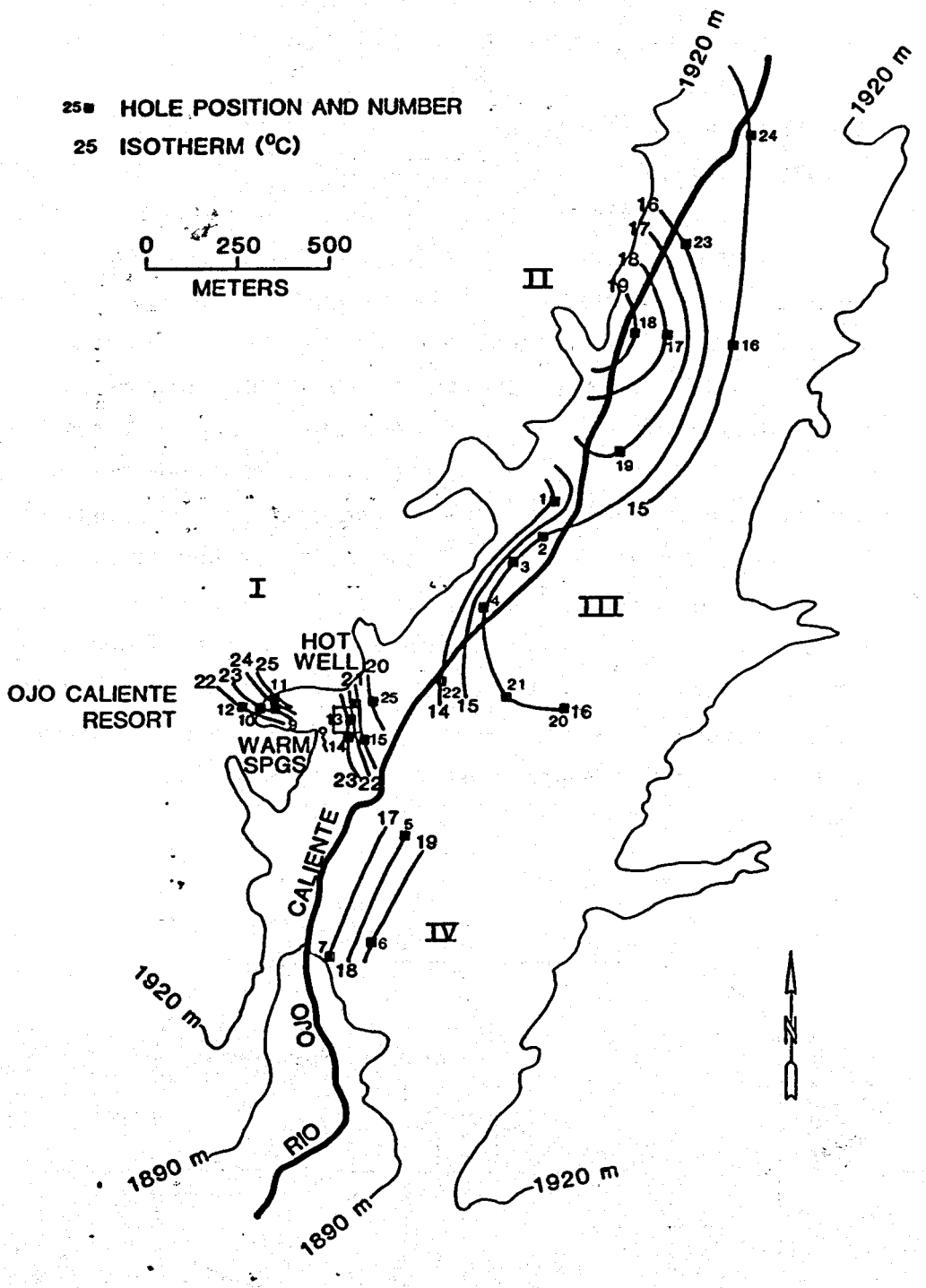

Fig. 14.
Shallow subsurface temperatures around Ojo Caliente. A network of 24 holes at a depth of 1.2±0.3 m and the average of three temperature measurements allowed pinpointing of four temperature anomalies (I-IV).

water because sediments saturated with geothermal fluids are much more conductive than sediments saturated with cold, fresh water.

9.1 Data Acquisition and Interpretation

A Schlumberger array consists of four co-linear electrodes, in which two closely spaced potential electrodes are centered between two current electrodes. A Schlumberger survey is conducted by increasing the current electrode separation between readings while leaving the potential electrodes fixed. During each reading the current between the outer electrodes and the potential drop between the inner electrodes is recorded. Figure 15 schematically shows the Schlumberger electrode configuration. Apparent resistivities are then calculated, which physically represent a normalized measure of the earth's resistivity after the effects of changing electrode spacings have been removed (Keller and Frischnect 1966). If the earth is horizontally layered, variations in effective resistivity as a function of current electrode separation can be used to infer resistivities as a function of depth below the array. The data are interpreted using a well-known computer program developed by Zohdy (1974). Figure 16 shows two sample Schlumberger sounding curves. The actual field measurements and values computed using Zohdy's program are tabulated in Table X.

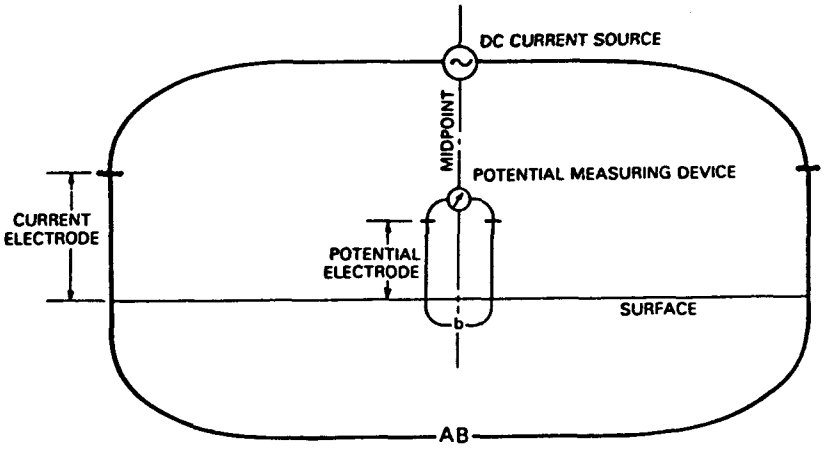

Fig. 15.
Schematic Schlumberger electrode configuration.

TABLE X

APPARENT RESISTIVITY DATA FOR OJO CALIENTE (Ωm)

AB/2 (m)	Stations								
	OJ1	OJ2	OJ3	OJ4	OJ5	OJ6	OJ7	OJ8	OJ9
1	65.0	15.2	318	52.5	-	71.1	22.6	28.3	22.5
1.46	79.8	19.8	354	40.5	-	85.5	22.9	34.2	23.1
2.15	94.0	28.8	348	34.0	-	105	27.1	41.4	26.4
3.16	103	39.9	307	33.6	42.4	112	33.1	50.1	32.5
4.64	105	54.0	241	34.7	40.6	113	40.6	60	38.4
6.82	106	65.3	164	36.6	40.7	108	47.0	67.9	45.5
10	103	69.2	111	38.1	44.4	97.3	52.5	67.1	52.0
14.6	95.7	67.0	75.5	37.8	50	79.6	51.9	59.3	50.4
21.5	81.3	57.8	51.2	31.6	47.5	54.1	46.3	47	46.5
31.6	60.7	42.2	34.7	29.3	40.0	29.4	37.9	34.5	37.3
46.4	46.0	27.1	23.4	18.1	29.6	20.1	28.2	25.9	27.2
68.2	38.9	22.4	15.8	15.7	22.5	17.8	17.5	23.8	19.2

9.2 Aquifer Properties

The formation resistivity ρ_F of a geothermal aquifer is related to the water resistivity ρ_W and the porosity ϕ by Archie's equation (1942)

$$\rho_F = 0.62\phi^{-2.15}\ \rho_W. \qquad (1)$$

Clearly, an increase in the resistivity of a sediment can be caused either by an increase in ρ_W or a decrease in ϕ. An increase in ρ_W implies a decrease of the ions concentration or of the pore water temperature. A change in the ionic concentration suggests mixing between cold dilute and thermomineral waters. Reduction of the formation temperature can also be caused by conductive cooling. Finally a porosity modification may be due either to lithologic variations or possibly by calcite deposition in the pore spaces of the rock, a common occurrence in low-to-moderate temperature geothermal areas.

9.3 Results

An electrically conductive zone has been found underneath the Rio Ojo Caliente valley with resistivities of less than 10 Ω-m. This zone is centered at line OJ 4 near the warm springs where it comes within 10 m of the surface (Fig. 17). This conductive zone deepens steadily to the north and south, disappearing 1 km to the north of the warm springs and 2 km to the south. The source of the thermal water apparently underlies the Ojo Caliente Resort adjacent to the warm springs, since the low resistivities ($\leq$10 Ω-m) are closest to the surface here. Thus, the geothermal fluids seem to rise as a plume from a segment of the Pliocene valley fault and then disperse eastward into the valley alluvium.

A zone of moderately conductive sediments (13-20 Ω-m) is encountered at intermediate depths (10-40 m) south of the warm springs. This may represent an outflow zone where thermal waters in the valley mix with fresh cool water. This area of mixing also may extend slightly to the north of Ojo Caliente. The more resistive sediments that overlie the conducting zones represent sediments saturated with cold fresh ground water fed by the Rio Ojo Caliente. Line OJ 8, run at the warm springs several hundred meters west of OJ 4, also

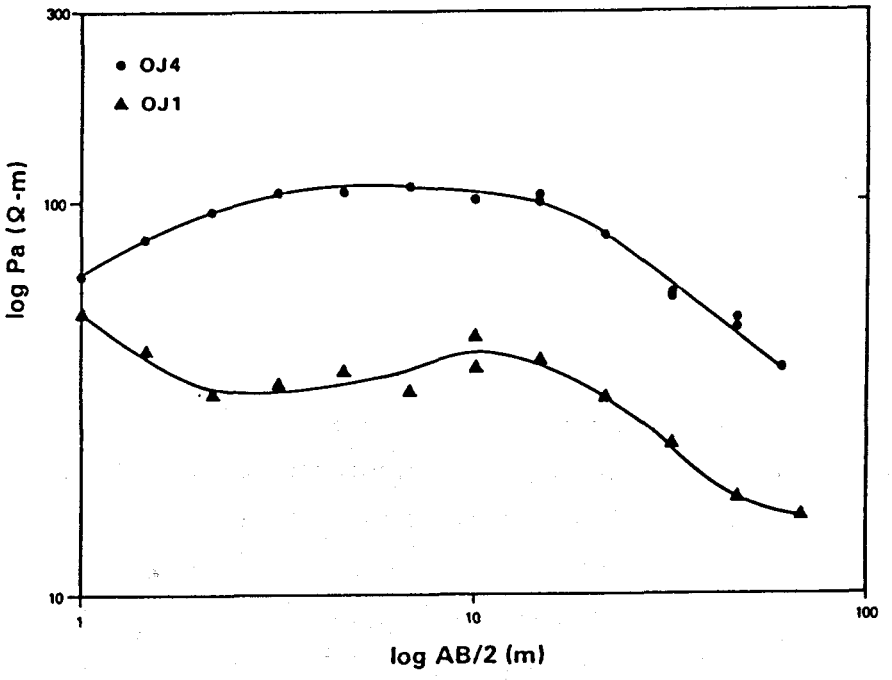

Fig. 16.
Two samples of Schlumberger sounding curves.

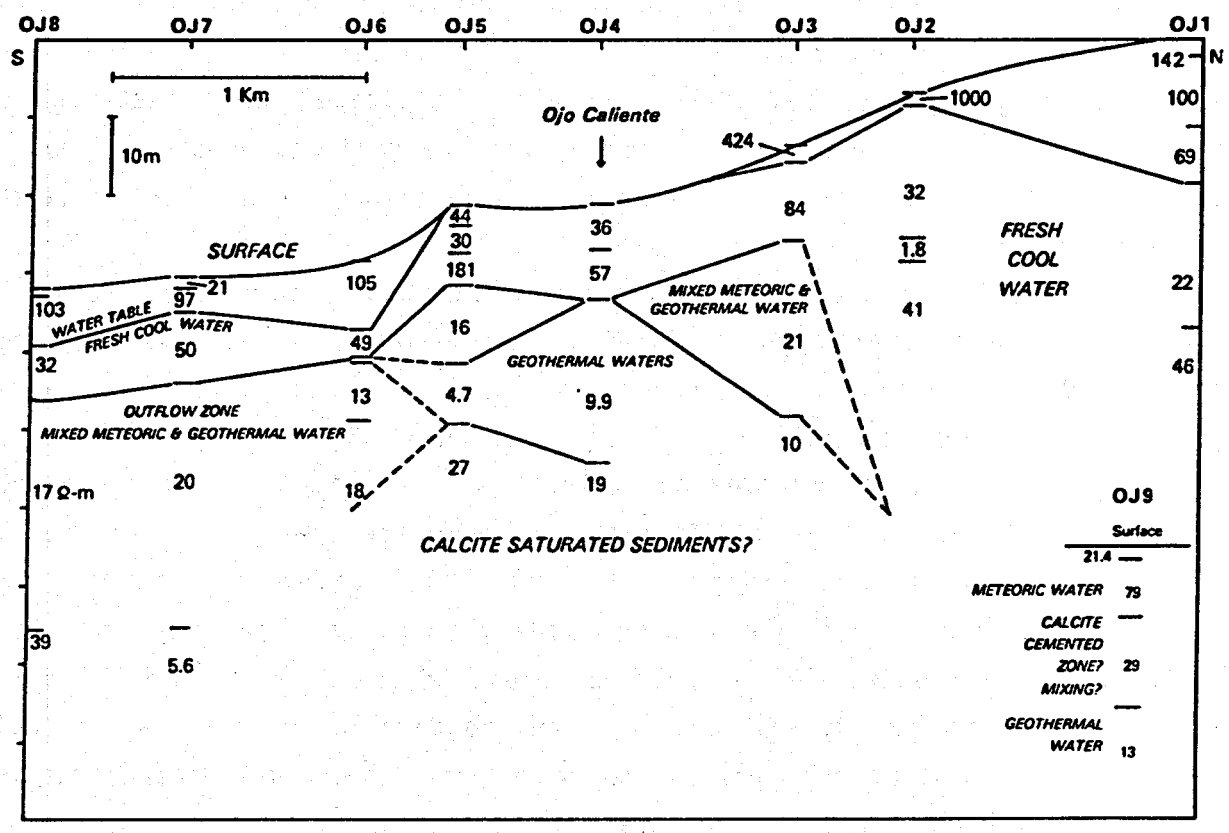

Fig. 17
Interpreted geoelectric north-south section of the Ojo Caliente valley alluvium.

detected the geothermal plume (Fig. 17). However, the slightly higher resistivities detected by OJ 8 may indicate calcite deposition in the underlying sediments due to loss of CO_2 from dissolved HCO_3. This reduces the porosity and thus increases the formation resistivity.

10. GEOTHERMAL POTENTIAL

10.1 Resources Assessment

The geologic study suggests that the Ojo Caliente thermal water system is structurally controlled and limited by faulting. No evidence of hydrothermally altered rocks allows one to think that a truly hot "reservoir" occurs at depth. Warm water circulation exists because of a sufficiently deep fissure network and the Rio Grande rift high heat flow province. Six heat flow measurements in a maximum radius of 47 km around Ojo Caliente average 114 mW/m^2

(New Mexico Energy Institute 1980), a typical value for a rift area and also twice as high as the world average of 60 mW/m^2 (Rybach, in Rybach and Muffler 1981). Locally present deposits of travertine indicate a past activity of Ca-HCO_3-rich waters probably from a more extensive regional geothermal system during the Quaternary. At the present time none of this concretion activity has been noticed.

Geochemical and hydrologic investigations have shown that at least 300-400 ℓ/min of thermal water at 55-60°C are available at relatively shallow depth (<100 m), whereas larger volumes of water might be tapped by deeper drill holes (200-400 m ?) at temperatures as high as 80-85°C. No evidence of important mixing between two types of water has been established for the warm springs and the Hot well at Ojo Caliente, despite the presence of the nearby river and the alluvium aquifer. However, the latter is contaminated extensively by the thermal water around the resort, as proven by the water supply wells and the shallow temperature holes. Chemical equilibria computations for the principal mineral phases allow one to think that the water would not create many scaling problems in the equipment of a future heat-extraction system as long as the system is operated as a closed loop.

A geophysical survey in the valley has emphasized the presence of thermo-mineral water in the shallow alluvium aquifer 2 km downstream from Ojo Caliente Resort and about 1 km upstream. This plume of geothermal water occupies an area of about 3 km^2 for a thickness of at least 10-20 m, according to the geoelectric section. Assuming an average thickness of 15 m, a mixing percentage of 30% of thermal water and an alluvium porosity of 30%, the total volume of thermal water spread into the aquifer reaches approximately $5 \cdot 10^6$ m^3. Because this aquifer is moving southward because of the topographic slope, there is a constant renewal of the water volumes. This implies a hidden source of thermal water discharging, which is likely to be much larger than the natural flow rate of the surface springs.

Around La Madera the group of springs with emergence temperatures $\leq$30°C does not have the same geothermal potential as the Ojo Caliente area. Deep temperatures probably do not exceed 40°C; therefore, the use of these waters for space heating is limited, except maybe for greenhouses fed by large flow rates or with the help of heat pumps (Gass 1982). Fish farming, balneology, and swimming pools are convenient uses for very low-temperature thermal water systems.

10.2 Recommendations

All these considerations favor further geothermal exploration for hot water resources at Ojo Caliente. Waters in the range of 60-80°C are very useful for many applications, but above all for space heating (buildings and greenhouses) and refrigeration. Of course, the other applications described for La Madera resources are also possible. To successfully tap the hot water, more detailed geophysical studies are needed along the hidden fault on the west side of the valley, 1 km upstream and downstream from Ojo Caliente Resort, to locate more precisely the main discharge zones into the alluvium. Anomaly II (Fig. 14) suggests that other hidden zones of warm water enter the alluvium besides those at the resort. Several 25- to 50-m-deep exploratory wells should be drilled along this southwest-northeast trend. Because of the dip and the width of the fissures, several wells on a line could be more productive than one very deep drill hole. It is also possible that hot water can be tapped efficiently from wells located in the middle of the valley, because of a downward staircase type of faulting underneath the alluvium.

Future production wells will need to be completed carefully to avoid any contamination with the shallow aquifer, which makes an interface with the ascending thermal water. This interface could be drawn down by extensive pumping. Therefore, cementation of the outer casing should continue through the alluvium and several meters below the contact with the metarhyolite, where packers should also be located. Slotted liners or screened tubing should not begin before the actual hot water production zone. Finally, it has to be pointed out that permanent pumping in new production wells at Ojo Caliente may certainly dry out the existing warm springs by lowering the artesian thermal water level. Thus, at an early stage of development, pumping tests in the new well(s) should monitor the discharge and other parameters of the warm springs. However, after the hot water (60-80°C) has flowed through a heat exchanger for space heating purposes, a large amount of warm water (40-60°C) will be available for swimming pools and medical uses in the spa.

ACKNOWLEDGMENTS

Much of this study has been possible thanks to the collaboration of George Mauro, owner of the Ojo Caliente Resort, who always welcomed us very kindly and patiently and gave us total freedom of investigation. The spring and well

owners around La Madera are also thanked for their cooperation, namely Joan Lowry, Don and Ernie Scharbag, and the Mesa Vista School. Pat Trujillo and Dale Counce, Los Alamos National Laboratory, analyzed all the water samples from 1979 to 1982 for the chemistry. Teledyne Isotopes, Westwood, New Jersey, carried out the tritium analyses, and the Centre d'Etudes Nucléaires de Saclay, Gif-sur-Yvette, France, took care of the stable isotopes. The carbon isotope analysis was performed by Dr. Austin Long, Laboratory of Isotope Geochemistry, University of Arizona. Thanks also to the numerous institutions and laboratories for the tritium data released through the WATSTORE data bank of the U.S. Geological Survey. Dr. Richard Jahns, Stanford University, generously let us examine an unpublished geologic map of his of the Ojo Caliente area. The late Mr. Verne Byrne provided stimulating discussion and helpful suggestions concerning the geology of the area. The authors are also grateful to the following persons from Los Alamos National Laboratory, who contributed in various ways to this study: Celestino Lucero introduced us to the community of Ojo Caliente; Jennifer East did early geologic mapping of the study area; Bernhard Hoffers helped during the resistivity soundings; Marcia Jones carried out a valuable work in typing and editing the manuscript; Anthony Garcia drew all the figures. Finally, the reviewers Grant Heiken and Ron Gooley are thanked for their critical comments of the manuscript.

REFERENCES

Archie, G. E., 1942, The electrical resistivity log as an aid in determining some reservoir characteristics, Trans. AIME 146, 54-62.

Arnórsson, S., 1975, Application of the silica geothermometer in low temperature hydrothermal areas in Iceland, Am. J. Sci. 275, 763-784.

Baldridge, W. S., P. E. Damon, M. Shafiqullah, and R. J. Bridwell, 1980, Evolution of the Rio Grande Rift, New Mexico: new potassium-argon ages, Earth Planet. Sci. Lett. 51, 309-321.

Barnes, I., and F. E. Clarke, 1969, Chemical properties of groundwater and their encrustation effects on wells, U.S. Geol. Surv. Prof. Paper 498-D, 58 pp.

Bureau of Land Management, 1978, Environmental assessment record and technical examination on proposed geothermal leasing in the Ojo Caliente area, Albuquerque District, EAR No. NM-010-8-33(G), 191 pp.

Clark, F. W., 1893, Report of the work done in the division of chemistry, U.S. Geol. Surv. Bull. 113, 115 pp.

Cope, E. D., 1875, Appendix 61. Report on the geology of that part of New Mexico surveyed during the field season of 1874, U.S. Geog. and Geol. Survey west of the 100th Meridian, p. 61-97, Appendix LL.

Craig, H., 1961, Isotopic variations in meteoric waters, Science 133:3465, 1702-1703.

Crook, J. K., 1899, The mineral waters of the United States and their therapeutic uses, Lea Bros. & Co., New York and Philadelphia, Pennsylvania, 588 pp.

Faler, K. T., K. L. Miyasako, and G. H. Wiegand, 1980, Long-term sub-surface temperature measurements along the Idaho Great Rift: a possible method for geothermal energy prospecting, J. Idaho Academy of Science, 16/1, 11-23.

Fouillac, C., G. Michard, M. Javoy, J. Jouzel, and L. Merlivat, 1976, Etude géochimique des sources thermominérales de Chateauneuf-les-Bains, J. Franç. Hydrol., 7, 3, no 21, 151-156.

Fouillac, C., and G. Michard, 1981, Sodium/lithium ratio in water applied to geothermometry of geothermal reservoirs, Geothermics 10:1, 55-70.

Fournier, R. O., 1973, Silica in thermal waters: laboratory and field investigation, Proc. Inter. Symp. Hydrogeochemistry and Biogeochemistry, Japan, 1970, Vol. 1, Hydrogeochemistry, Washington, DC, J. W. Clark, 122-139.

Fournier, R. O., 1977, Chemical geothermometers and mixing models for geothermal systems, Geothermics 5:1-4, 41-50.

Fournier, R. O., 1979, A revised equation for the Na/K geothermometer, Geoth. Res. Coun. Trans. 3, 221-224.

Fournier, R. O., and J. J. Rowe, 1966, Estimation of underground temperatures from the silica content of water from hot springs and wet-steam wells, Am. J. Sci. 264, 685-697.

Fournier, R. O., and A. H. Truesdell, 1973, An empirical Na-K-Ca geothermometer for natural waters, Geochim. Cosmochim. Acta 37, 1255-1275.

Fournier, R. O., and R. W. Potter, 1979, Magnesium correction to the Na-K-Ca chemical geothermometer, Geochim. Cosmochim. Acta 43, 1543-1550.

Freeze, R. A., and J. A. Cherry, 1979, Groundwater, Prentice-Hall Inc., Englewood Cliffs, NJ, 604 pp.

Fritz, P., and J. Ch. Fontes (eds), 1980, Handbook of Environmental Isotope Geochemistry, Vol. 1A: The Terrestrial Environment, Elsevier, Amsterdam, 545 pp.

Garrels, R. M., and R. M. Dreyer, 1952, Mechanism of limestone replacement at low temperatures and pressures, Geol. Soc. Am. Bull. 63, 325-379.

Gass, T. E., 1982, The geothermal heat pump, Geoth. Res. Coun. Bull. 11:11, 3-8.

Goff, F., T. McCormick, P. Trujillo, D. Counce, and C. Grigsby, 1982, Geochemical data for 95 thermal and nonthermal waters of the Valles Caldera-Southern Jemez Mountains Region, New Mexico, Los Alamos National Laboratory report LA-9367-OBES, 51 pp.

Goff, F., T. McCormick, J. N. Gardner, P. E. Trujillo, D. A. Counce, R. Vidale, and R. Charles, 1983, Water geochemistry of the Lucero Uplift, New Mexico - A geothermal investigation of low-temperature mineralized fluids, Los Alamos National Laboratory report LA-9738-OBES, 26 pp.

Grigsby, C. O., J. W. Tester, P. E. Trujillo, D. A. Counce, J. Abbott, C. E. Holley and L. A. Blatz, 1983, Rock-water interactions in hot dry rock geothermal systems: field investigations of in situ geochemical behavior, in G. Heiken and F. Goff (eds.) Geothermal energy from Hot Dry Rock, J. Volcanol. Geotherm. Energy Res. 15, 101-136.

Jones, F. A., 1904, New Mexico Mines and Minerals, New Mexico Printing Co., Santa Fe, 349 pp.

Keller, G. V., and F. C. Frischnect, 1966, Electrical Methods in Geophysical Prospecting, Pergamon Press, New York, 95 pp.

Kharaka, Y. K., and I. Barnes, 1973, SOLMNEQ: Solution-Mineral Equilibrium Computations, U.S. Geol. Surv. Computer Contrib., U.S. Dept. Commerce, NTIS report PB-215899, 82 pp.

Kruseman, G. P., and N. A. De Ridder, 1979, Analysis and evaluation of pumping test data, Inter. Inst. for Land Reclamation and Improvement (ILRI), Wageningen, The Netherlands, Bull. 11, 200 pp.

Loew, O., 1875, Report upon mineralogical, agricultural, and chemical conditions observed in portions of Colorado, New Mexico, and Arizona, U.S. Geog. and Geol. Survey west of the 100th Meridian, Wheeler, G. M., v. 3, pp. 613-627.

Manley, K., 1981, Redefinition and description of the Los Piños Formation of north-central New Mexico, Geol. Soc. of Am. Bull. 92, 984-989.

May, S. J., 1979, Neogene stratigraphy and structure of the Ojo Caliente-Rio Chama area, Española Basin, New Mexico, N.M. Geol. Soc. Guidebk., 30th Field Conf., Santa Fe Country, 1979, 83-88.

May, S. J., 1980, Neogene geology of the Ojo Caliente-Rio Chama area, Española Basin, New Mexico, Ph.D. dissertation, Univ. of New Mexico, Albuquerque, 205 pp.

New Mexico Energy Institute, 1980, Geothermal resources of New Mexico, Map, scale 1:500 000 produced by Nat. Geophys. and Solar-Terrest. Data Center and by Nat. Ocean. and Atmosph. Administr.

Peale, A. V., 1886, List and analysis of the mineral springs of the United States, U.S. Geol. Surv. Bull. 32.

Rybach, L., and L. J. P. Muffler (eds.) 1981, Geothermal Systems, Principles and Case Histories, Wiley, New York, 359 pp.

Stearns, N. D., Stearns, H. T., and Waring, G. A., 1937, Thermal Springs in the United States, U.S. Geol. Surv. Water-Supply Paper 679-B.

Stix, J., C. Pearson, F. D. Vuataz, F. E. Goff, J. East, and B. Hoffers, 1982, Geology, resistivity and hydrogeochemistry of the Ojo Caliente Hot Springs area, northern New Mexico, Geotherm. Res. Coun. Trans. 6, 55-58.

Summers, W. K., 1976, Catalog of thermal waters in New Mexico, N.M. Bur. Mines Miner. Res., Hydrol. Report 4, 80 pp.

Tardy, Y., 1980, Géochimie des interactions entre les eaux, les minéraux et les roches, S.A.R.L. Eléments, Tarbes, 239 pp.

Trainer, F. W., and F. P. Lyford, 1979, Geothermal hydrology in the Rio Grande rift, north-central New Mexico, N.M. Geol. Soc. Guidebook, 30th Field Conf., Santa Fe Country, 229-306.

Treiman, A. H., 1977, Precambrian geology of the Ojo Caliente quadrangle, Rio Arriba and Taos Counties, New Mexico, M.S. thesis, Stanford Univ., Palo Alto, California, 93 pp.

Ungemach, P., 1982, Development of low grade geothermal resources in the European Community - present status - problem areas - future prospects, Int. Conf. Geothermal Energy, Florence, Italy, G1, 1-41.

U.S. Geological Survey, 1981, Water Resources Data for New Mexico, Water Year 1980, USGS/WRD/HD-81/086, 679 pp.

Vuataz, F. D., 1982, Hydrogéologie, géochimie et géothermie des eaux thermales de Suisse et des régions alpines limitrophes, Matér. Géol. Suisse, Sér. Hydrol. 29, Kümmerly & Frey, Berne, 174 pp.

Vuataz, F. D., J. F. Schneider, F. C. Jaffé, and E. Mazor, 1983, Hydrogeochemistry and extrapolation of end-members in a mixed thermal water system, Vals, Switzerland, Eclogae geol. Helv., 76/2, 431-450.

Walton, W. C., 1970, Groundwater resource evaluation, McGraw Hill, New York, 664 pp.

WATSTORE, 1983, Water Data Storage and Retrieval System, U.S. Geological Survey, Albuquerque, N.M.

White, D. E., 1970, Geochemistry applied to the discovery, evaluation and exploitation of geothermal energy resources, Geothermics, Special Issue 2:1, 58-80.

Zohdy, A. A. R., 1974, Automatic interpretation of Schlumberger sounding curves using modified Dar Zarrouk functions, U.S. Geol. Surv. Bull. 1313-E.

☆U.S. GOVERNMENT PRINTING OFFICE: 1984-0-776-026/4068

DO NOT MICROFILM
THIS PAGE

Printed in the United States of America
Available from
National Technical Information Service
US Department of Commerce
5285 Port Royal Road
Springfield, VA 22161

Microfiche (A01)

Page Range	NTIS Price Code
001-025	A02
026-050	A03
051-075	A04
076-100	A05
101-125	A06
126-150	A07
151-175	A08
176-200	A09
201-225	A10
226-250	A11
251-275	A12
276-300	A13
301-325	A14
326-350	A15
351-375	A16
376-400	A17
401-425	A18
426-450	A19
451-475	A20
476-500	A21
501-525	A22
526-550	A23
551-575	A24
576-600	A25
601-up*	A99

*Contact NTIS for a price quote.

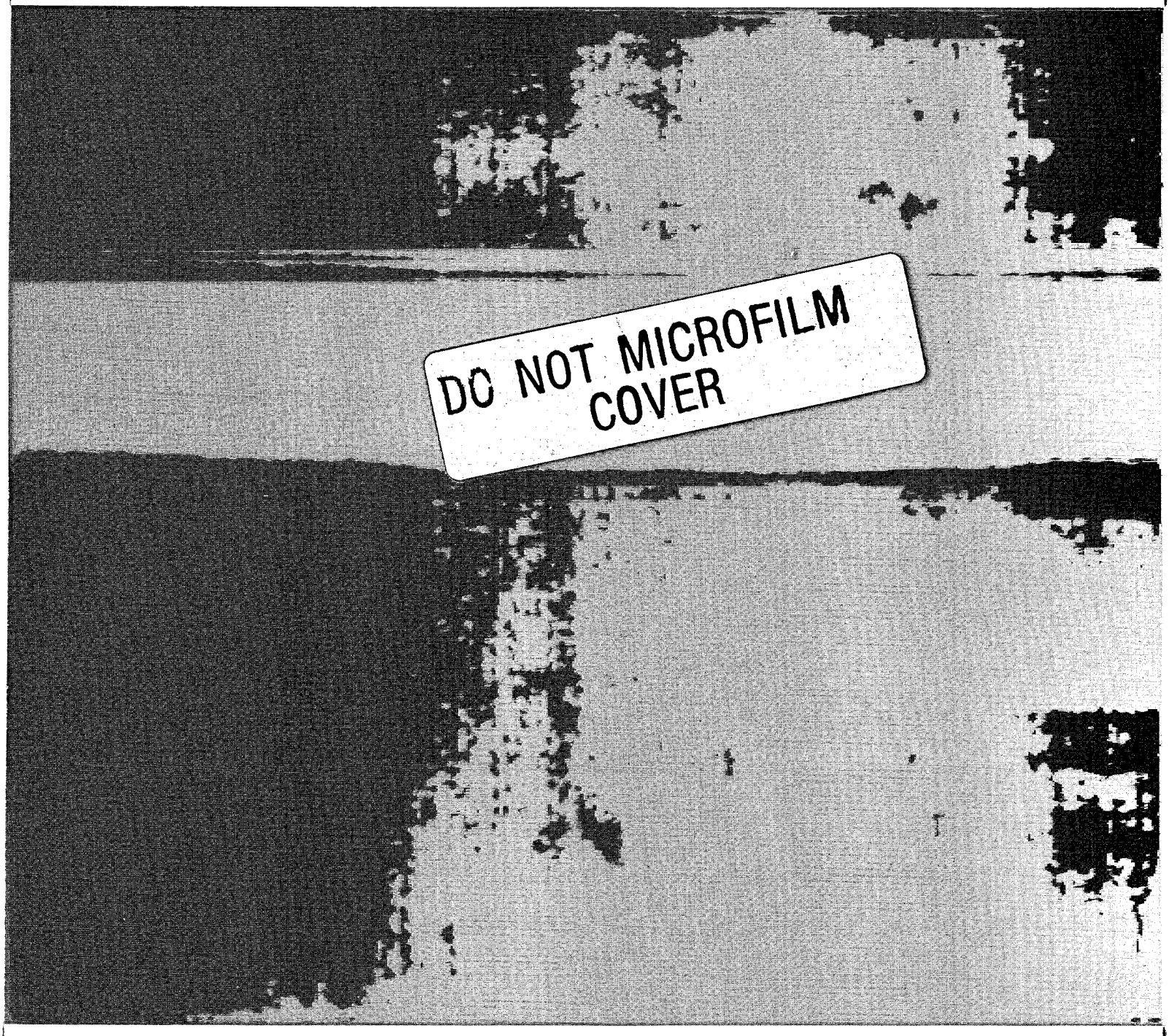

Los Alamos